PLASMA SURFACE TREATMENT OF PPS/CF THERMOPLASTIC COMPOSITE LAMINATES TO IMPROVE THEIR FILM ADHESIVE JOINING PERFORMANCE

A THESIS SUBMITTED TO
THE GRADUATE SCHOOL OF NATURAL AND APPLIED SCIENCES
OF
MIDDLE EAST TECHNICAL UNIVERSITY

BY

ADEM CAN UŞAK

IN PARTIAL FULFILLMENT OF THE REQUIREMENTS
FOR
THE DEGREE OF MASTER OF SCIENCE
IN
METALLURGICAL AND MATERIALS ENGINEERING

JULY 2023

Approval of the thesis:

PLASMA SURFACE TREATMENT OF PPS/CF THERMOPLASTIC COMPOSITE LAMINATES TO IMPROVE THEIR FILM ADHESIVE JOINING PERFORMANCE

submitted by **ADEM CAN UŞAK** in partial fulfillment of the requirements for the degree of **Master of Science** i**n Metallurgical and Materials Engineering, Middle East Technical University** by,

Prof. Dr. Halil Kalıpçılar
Dean, Graduate School of **Natural and Applied Sciences** _____

Prof. Dr. Ali Kalkanlı
Head of the Department, **Metallurgical and Materials Eng.** _____

Prof. Dr. Cevdet Kaynak
Supervisor, **Metallurgical and Materials Eng., METU** _____

Examining Committee Members:

Assoc. Prof. Dr. Batur Ercan
Metallurgical and Materials Eng., METU _____

Prof. Dr. Cevdet Kaynak
Metallurgical and Materials Eng., METU _____

Assist. Prof. Dr. Salih Ertan
Chemical Eng., Atılım University _____

Assist. Prof. Dr. Yusuf Keleştemur
Metallurgical and Materials Eng., METU _____

Assist. Prof. Dr. Şeniz Uçar
Metallurgical and Materials Eng., METU _____

Date: 31.07.2023

I hereby declare that all information in this document has been obtained and presented in accordance with academic rules and ethical conduct. I also declare that, as required by these rules and conduct, I have fully cited and referenced all material and results that are not original to this work.

Name Last name : Adem Can Uşak

Signature :

ABSTRACT

PLASMA SURFACE TREATMENT OF PPS/CF THERMOPLASTIC COMPOSITE LAMINATES TO IMPROVE THEIR FILM ADHESIVE JOINING PERFORMANCE

Uşak, Adem Can
Master of Science, Metallurgical and Materials Engineering
Supervisor: Prof. Dr. Cevdet Kaynak

July 2023, 73 pages

The main purpose of this study was to observe the degree of the improvement on the Film Adhesive joining performance of Poly(phenylene sulfide) / Carbon Fiber (PPS/CF) thermoplastic composite laminates when their surfaces were treated by Atmospheric Plasma technique. For this purpose, plasma treated surfaces were compared with Untreated and the traditional Grit-blasted surfaces.

Treated surfaces were characterized by various techniques including Contact Angle, Surface Energy, Surface Roughness, FTIR and XPS analyses. Then, joining performance of the PPS/CF composite samples bonded by an epoxy-based film adhesive was determined by using three different mechanical tests; Single-lap shear strength, Mode-I interlaminar fracture toughness energy, and drop-weight impact toughness.

Grit-blasting surface treatment increased surface roughness of the specimens enormously, leading to mechanical interlocking as the dominant bonding mechanism. Contrarily, plasma surface treatment resulted in formation of chemically reactive sites, thus dominant bonding mechanisms in the Film Adhesive joining were certain polar interactions and chemical bonding.

Mechanical tests pointed out that compared to Grit-blasting, Plasma surface treatment resulted in considerably higher joint performance regarding Interlaminar Shear Strength, Interlaminar Fracture Toughness and Impact Toughness, with the Cohesive failure mode. Accordingly, it could be stated that traditional Grit-blasting could be replaced with Plasma surface treatment before Film Adhesive joining of PPS/CF composite parts in aircraft industry.

Keywords: Poly(phenylene sulfide), Carbon Fiber, Plasma Surface Treatment, Grit-blasting surface treatment, Film Adhesive Joining.

ÖZ

PLAZMA YÜZEY İŞLEMİ İLE PPS/CF TERMOPLASTİK KOMPOZİT LAMİNATLARIN FİLM YAPIŞTIRICI İLE BİRLEŞTİRME PERFORMANSININ ARTIRILMASI

Uşak, Adem Can
Yüksek Lisans, Metalurji ve Malzeme Mühendisliği
Tez Yöneticisi: Prof. Dr. Cevdet Kaynak

Temmuz 2023, 73 sayfa

Bu çalışmanın temel amacı Poli(fenilen sülfit) / Karbon Elyaf (PPS/CF) termoplastik kompozit laminatların yüzeyleri Atmosferik Plazma tekniği ile işlendiğinde Film Yapıştırıcı ile birleştirme performansındaki iyileşme derecesini gözlemlemekti. Bu amaçla, plazma uygulanmış yüzeyler, İşlenmemiş ve geleneksel Grit-kumlanmış yüzeylerle karşılaştırılmıştır.

İşlem görmüş yüzeyler, Temas Açısı, Yüzey Enerjisi, Yüzey Pürüzlülüğü, FTIR ve XPS analizleri gibi çeşitli tekniklerle karakterize edilmiştir. Daha sonra epoksi bazlı film yapıştırıcı ile yapıştırılan PPS/CF kompozit numunelerin birleştirme performansları üç farklı mekanik test kullanılarak belirlenmiştir; Tek-tesirli kayma mukavemeti, Mod-I tabakalar arası kırılma tokluğu enerjisi ve ağırlık düşürme darbe tokluğu.

Grit-kumlama yüzey işlemi, numunelerin yüzey pürüzlülüğünü büyük ölçüde arttırdı ve bu da baskın bağlanma mekanizması olarak mekanik kilitlemeye yol açtı. Aksine, plazma yüzey işlemi, kimyasal olarak reaktif bölgelerin oluşmasına neden oldu, bu nedenle, Film Yapıştırıcı birleştirmede baskın bağlanma mekanizmaları, belirli polar etkileşimler ve kimyasal bağlardı.

Mekanik testler, Grit-kumlama ile karşılaştırıldığında, Plazma yüzey işleminin, Katmanlar Arası Kayma Dayanımı, Katmanlar Arası Kırılma Tokluğu ve Darbe Tokluğu açısından, Kohezyon kırılma modu ile önemli ölçüde daha yüksek bağlantı performansıyla sonuçlandığını göstermiştir. Buna göre, uçak endüstrisinde PPS/CF kompozit parçaların Film Yapıştırıcı ile birleştirilmesinden önce geleneksel Grit-kumlama işleminin yerini Plazma yüzey işlemine bırakabileceği söylenebilir.

Anahtar Kelimeler: Poli(fenilen sülfür), Karbon Elyaf, Plazma Yüzey İşlemi, Grit-kumlama Yüzey İşlemi, Film Yapıştırıcı ile Birleştirme.

To my family.

ACKNOWLEDGMENTS

First of all, I would like to convey my special thanks to my advisor Prof. Dr. Cevdet Kaynak for his endless support, guidance and efforts throughout the thesis study and my entire graduate program. I also would like to express my appreciation for his patience and understanding in the compelling time of pandemic.

I would like to express my gratitude to the examining committee, Assoc. Prof. Dr. Batur Ercan, Assist. Prof. Dr. Salih Ertan, Assist. Prof. Dr. Yusuf Keleştemur and Assist. Prof. Dr. Şeniz Uçar for their precious evaluation and recommendations during my thesis defense period of time.

I would like to express my profound gratitude to Materials Engineering Department at Turkish Aerospace for providing me with the resources, guidance, and professional environment necessary to conduct my research. I also would like to express my heartfelt gratitude to my colleagues at Turkish Aerospace, Alp Aykut Kibar, Ege Demir, Seda Turan, Münevver Eryılmaz, Mertcan Köçer, Esra Özçelik, Ayşe Hande Çalış, Polatcan Çakıroğlu, Bahri Söyleyici, Seyit Ali Örsel, Ahmetcan Alkoç, İbrahim Aydoğan, Mehmet Oruç and Oğuzhan Yavuz for their endless contribution, expertise, and encouragement in the field of practice. I would like to extend my sincere appreciation to my dear friends, Barış Berka Özdaş, Doğukan Göktürk Mezda, Baran Doğan, Özgür Uyar and Merve Atlıoğlu for their invaluable supports to my study.

I would like to state thankfulness to my beloved family members, Abdullah, Nurhan, Sevim and Nida. I am forever indebted to their endless support, encouragement, and unwavering belief in my abilities. Additionally, I extend my heartfelt thanks to my grandfather for his positive motivation during my academic journey. I will proudly carry your name throughout my life.

Lastly, I am profoundly thankful for Başaknaz whose wholehearted support has been my source of guiding light in this journey. Her soul will always be my eternal whispers of inspiration.

TABLE OF CONTENTS

ABSTRACT v

ÖZ vii

ACKNOWLEDGMENTS x

TABLE OF CONTENTS xii

LIST OF TABLES xiv

LIST OF FIGURES xv

NOMENCLATURE xviii

CHAPTERS

1 INTRODUCTION 1

1.1 Thermoplastic Matrix Composite Laminates 1

1.2 Joining Methods of Thermoplastic Matrix Composite Structures 3

1.3 Joining by Using Film Adhesives 6

1.4 Surface Treatments Used Before Film Adhesive Joining Method 8

1.5 Literature Review 12

1.6 Aim of the Thesis 14

2 EXPERIMENTAL WORK 15

2.1 Production of PPS/CF Laminates to be Surface Treated and then Joined 15

2.2 Surface Treatments of PPS/CF Laminates Before Joining 19

2.3 Analyses of Surface Treated PPS/CF Laminates Before Joining 21

2.4 Joining of PPS/CF Laminates with Film Adhesive Bonding 25

2.5 Mechanical Testing of the Film Adhesive Joined Specimens 27

3 RESULTS AND DISCUSSION 31

3.1 Selection of Plasma Treatment Parameters by Thermal Camera Analysis..31

3.2 Changes in the Roughness of Treated PPS/CF Surfaces 34
3.3 Changes in the Wettability of Treated PPS/CF Surfaces 36
3.4 Changes in the Chemistry of Treated PPS/CF Surfaces 39
3.5 Structural Integrity and Matrix Crystallinity of PPS/CF Laminates Before and After Joining 45
3.6 Effects of Plasma Treatment on the Interlaminar Shear Strength of Joined Specimens 49
3.7 Effects of Plasma Treatment on the Interlaminar Fracture Toughness of Joined Specimens 53
3.8 Effects of Plasma Treatment on the Drop-Weight Impact Toughness of Joined Specimens 57
4 CONCLUSIONS 63
REFERENCES 65

LIST OF TABLES

TABLES

Table 3.1 Specimen Designation and values of the Plasma Velocity and Plasma Distance parameters selected for each one; and average values of the Surface Temperatures recorded by Thermal Camera. 32

Table 3.2 Average Surface Roughness values in terms of *Ra* and *Rz* for the Untreated and treated PPS/CF surfaces. 35

Table 3.3 Average values of the Water Contact Angle and Total Surface Free Energy including its Polar and Dispersion Components of Untreated and Treated PPS/CF surfaces. 37

Table 3.4 XPS Elemental Compositions (C, O, S, N) including O/C and O/S Atomic Ratios of the Untreated, Grit-blasted and Plasma Treated PPS/CF Surfaces. 42

Table 3.5 Average values of the Interlaminar Shear Strength and Interlaminar Fracture Toughness Energy of the Specimens “after” joining. 53

Table 3.6 Values of the Dent Depth, Damage Area, Maximum Contact Force (F_{max}) and Maximum Absorbed Energy (E_{max}) obtained from Drop-Weight Impact tests of Untreated, Grit-blasted and Plasma Treated PPS/CF specimens “after” joining. 60

LIST OF FIGURES

FIGURES

Figure 1.1 (a) Monomer structure of the PPS matrix, (b) 5HS weave style of the Carbon Fiber reinforcement. 2
Figure 1.2 Schematics of the Joining Methods used for Thermoplastic Matrix Composite Structures all under Pressure. 4
Figure 1.3 Schematics of the Film Adhesive Joining method and three Bonding Mechanisms that might occur. 7
Figure 1.4 (a) Schematic of a typical Grit-blasting system, (b) manual application for large structures. 10
Figure 1.5 Schematic of the Atmospheric Plasma surface Treatment. 12
Figure 2.1 Steps during production of PPS/CF composite laminates; (a) cutting of one prepreg layer from the roll, (b) stacking and hot press consolidation of the five prepreg layers, (c) 1.5 mm thick laminates produced, (d) ultrasonic inspection of the produced laminates, (e) cutting of the laminates into certain sizes required, and (f) DSC analysis of the laminate samples. 18
Figure 2.2 Grit-blasting and cleaning of PPS/CF laminate surfaces, and their appearance before and after the treatment. 19
Figure 2.3 Atmospheric plasma surface treatment of PPS/CF laminates and protection of the treated surfaces until joining process..... 21
Figure 2.4 Analyses used to characterize untreated and treated PPS/CF laminate surfaces before joining; (a) Thermal Camera, (b) Surface Roughness, (c) and (d) Wettability-Contact Angle, (e) FTIR and (f) XPS. 24
Figure 2.5 Joining of PPS/CF laminates with Film Adhesive; (a) Peeling-off the Film Adhesive from carrier films and cutting, (b) Placing the Film Adhesive in between the two laminates, (c) Plastic vacuum bagging, (d) Autoclave curing, (e) Laminate after joining, and (f) Mechanical test specimens extracted from joined laminates. 26

Figure 2.6 Loading fixture and specimen geometry of the mechanical tests used for joining performance; (a) Single-Lap Shear Strength, SLSS, (b) Mode-I Interlaminar Fracture Toughness, *GIc* and (c) Drop-Weight Impact Toughness. 30
Figure 3.1 Schematics of Thermal Camera analysis, and an example of temperature mapping image obtained during plasma treatment of PPS/CF surfaces. 33
Figure 3.2 Effects of Grit-blasting and Plasma Treatments on the Surface Roughness (*Ra* and *Rz*) of PPS/CF specimens. 35
Figure 3.3 Effects of Grit-Blasting and Plasma Treatments on the Water Contact Angle and Total Surface Free Energy including its Polar and Dispersion Components of PPS/CF surfaces. 38
Figure 3.4 FT-IR spectra of the Untreated, Grit-Blasted and one of the Plasma Treated (Plz-V10-D11) PPS/CF surfaces. 40
Figure 3.5 XPS spectra of the Untreated, Grit-blasted and one of the Plasma Treated (Plz-V10-D11) PPS/CF surfaces. 43
Figure 3.6 Deconvoluted forms of the C 1s and S 2p XPS spectra for the Untreated sample (above) and Plz-V10-D11 Plasma treated sample (below) 44
Figure 3.7 Examples of the Ultrasonic Inspection images of the PPS/CF laminates "before" joining, and "after" joining of Untreated, Grit-blasted and Plasma treated surfaces. 46
Figure 3.8 First Heating and Cooling DSC Thermograms of PPS/CF samples before and after Joining. 48
Figure 3.9 Load-Displacement curves and SLSS values of the Untreated, Grit-blasted and Plasma treated PPS/CF specimens after joining. 50
Figure 3.10 Schematics of Three Typical Interlaminar Failure Modes that could be observed in Film Adhesive Joining method. 51
Figure 3.11 Examples of the three typical interlaminar failure modes observed during SLSS tests. 52
Figure 3.12 Load-Displacement curves and G_{IC} values of the Untreated, Grit-blasted and Plasma treated PPS/CF specimens after joining. 55

Figure 3.13 Examples of the three typical interlaminar failure modes observed during G_{IC} tests. 56
Figure 3.14 Examples of the "Contact Force versus Time" and "Absorbed Energy versus Time" curves obtained during Drop-Weight Impact tests of PPS/CF specimens after joining. 59
Figure 3.15 Maximum Contact Force (F_{max}) and Maximum Absorbed Energy (E_{max}) of the Untreated, Grit-blasted and Plasma treated PPS/CF specimens after Joining. 60
Figure 3.16 Examples of the Top-View Photographic Images taken under visible light (left) and UV light (right) of the Damage Zones occurred in the Drop-Weight Impact tests of PPS/CF specimens after joining. 61
Figure 3.17 Examples of the through-thickness Ultrasonic Images together with Image Analyses Software area determination of the Damage Zones occurred in the Drop-Weight Impact tests of the PPS/CF specimens after joining. 62

NOMENCLATURE

ASTM	American Society for Testing and Materials
atm	Atmosphere
ATR	Attenuated Total Reflectance
AUTT	Automated Ultrasonic Through Transmission
CF	Carbon Fiber
cps	Count Per Second
D	Nozzle-Surface Distance
DSC	Differential Scanning Calorimetry
EN	European Technical Standards
eV	Binding Energy
F	Force (Load)
FTIR	Fourier-transform Infrared
GF	Glass Fiber
GSM	Gram per Square Meter
G_{IC}	Interlaminar Fracture Toughness Mode-I
ISO	International Organization for Standardization
J	Joule
kN	Kilonewton
MPa	Mega Pascal
P	Pressure
PAEK	Poly(aryletherketone)
PEEK	Poly(etheretherketone)
PEKK	Poly(etherketoneketone)
Plz	Plasma
PMC	Polymer Matrix Composite

PP	Polypropylene
PPS	Poly(phenylenesulfide)
Ra	Average Roughness
Rz	Height of Roughness
SLSS	Single-lap Shear Strength
T_c	Crystallization Temperature
T_g	Glass-transition Temperature
T_m	Melting Temperature
UV	Ultraviolet
V	Plasma Velocity
wt	Weight
X_c	The Degree of Crystallinity
XPS	X-ray Photoelectron Spectroscopy
ZnSe	Zinc Selenide
θ	Contact Angle
γ_l	Total Surface Tension of Liquid
γ_s	Total Surface Tension of Solid
γ^d	Dispersion Components
γ^p	Polar Components
5HS	Five Harness-Satin

CHAPTER 1

INTRODUCTION

Polymer matrix composite (PMC) materials are widely used in all sectors, the pioneer one being aerospace industry because they offer high mechanical performance with low density. Depending on the matrix type, PMC materials are classified into two classes as thermoset and thermoplastic matrix composites. Even tough thermoset matrix composites are still being used in the field of aerospace for many components, the recent trend is to replace these parts with thermoplastic matrix composites in order to overcome certain disadvantages of thermoset matrices.

1.1 Thermoplastic Matrix Composite Laminates

Main shortcomings of the thermoset matrices could be listed as; no reusability, complicated curing procedures of the liquid resin, and the necessity of sub-zero storage conditions leading to limited shelf-life.

Thermoplastic matrices require no curing, no cold storage; they could be shaped by applying certain levels of temperature and pressure, with the advantage of re-shaping.

Of course, for the high performance aircraft parts, ordinary commodity thermoplastics could not be used, it would be wise to use engineering thermoplastics having higher glass transition temperature values and higher partial crystallinity degree. From this perspective, the most widely preferred thermoplastic matrices in aerospace industry are; poly(etheretherketone) (PEEK), poly(etherketoneketone) (PEKK), poly(aryletherketone) (PAEK) and poly(phenylenesulfide) (PPS).

In this study, the composite system has PPS matrix. As shown in Figure 1.1 (a), monomer structure of PPS is composed of aromatic ring attached to the sulfide element leading to higher thermal resistance and mechanical performance including toughness.

Reinforcement fibers play a very critical role in the performance of polymer matrix composites because the load is transferred from the matrix to the fibers. Although several continuous fiber types are available such as glass and aramid, carbon fibers are primarily preferred in the structural aerospace parts. Continuous fibers could be used as unidirectional or woven forms, which are available in various weave styles such as plain wave and different satin waves. For the ease of composite part manufacturing, thermoplastic matrices and these continuous fiber forms are normally combined before. These matrix-fiber combination systems available in the market are named as “pre-pregs”. When certain number of these prepreg layers are consolidated, then they are named as “laminates”.

In this study, for the production of laminates, pre-pregs used has PPS matrix reinforced with woven carbon fibers (CF) with 5-harness satin (5HS) weave style (Figure 1.1 (b)).

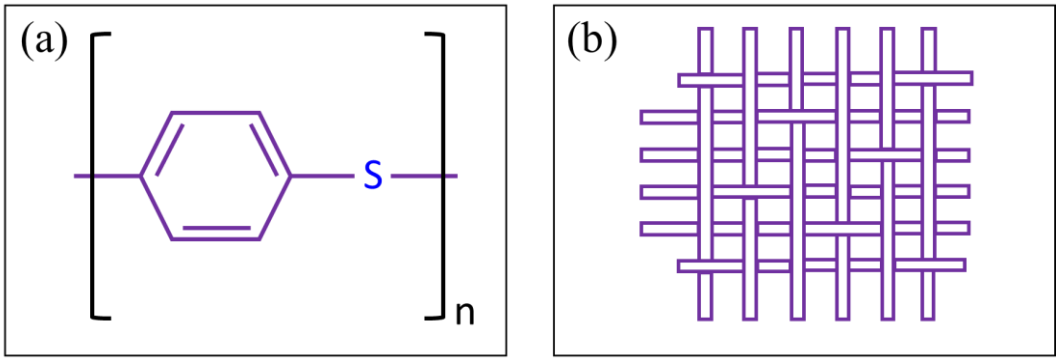

Figure 1.1 (a) Monomer structure of the PPS matrix, (b) 5HS weave style of the Carbon Fiber reinforcement.

1.2 Joining Methods of Thermoplastic Matrix Composite Structures

In the aircraft industry, methods used to join thermoplastic matrix composite structures can be categorized into three classes; mechanical fastening, co-consolidation & welding, and adhesive bonding. Joining mechanism of each one are illustrated in Figure 1.2.

(i) *Mechanical Fastening*

In this method, parts are joined mechanically by using various forms of fasteners (e.g. screws, rivets, pins, staples, etc.) usually made of stainless steel or titanium and aluminum alloys. Main problems encountered in this method are; increase in the product weight, thermal expansion coefficient mismatch between the composite and the fastener, fastener holes acting as stress concentrators, and discontinuity in the load carrying capacity of the fiber reinforcements.

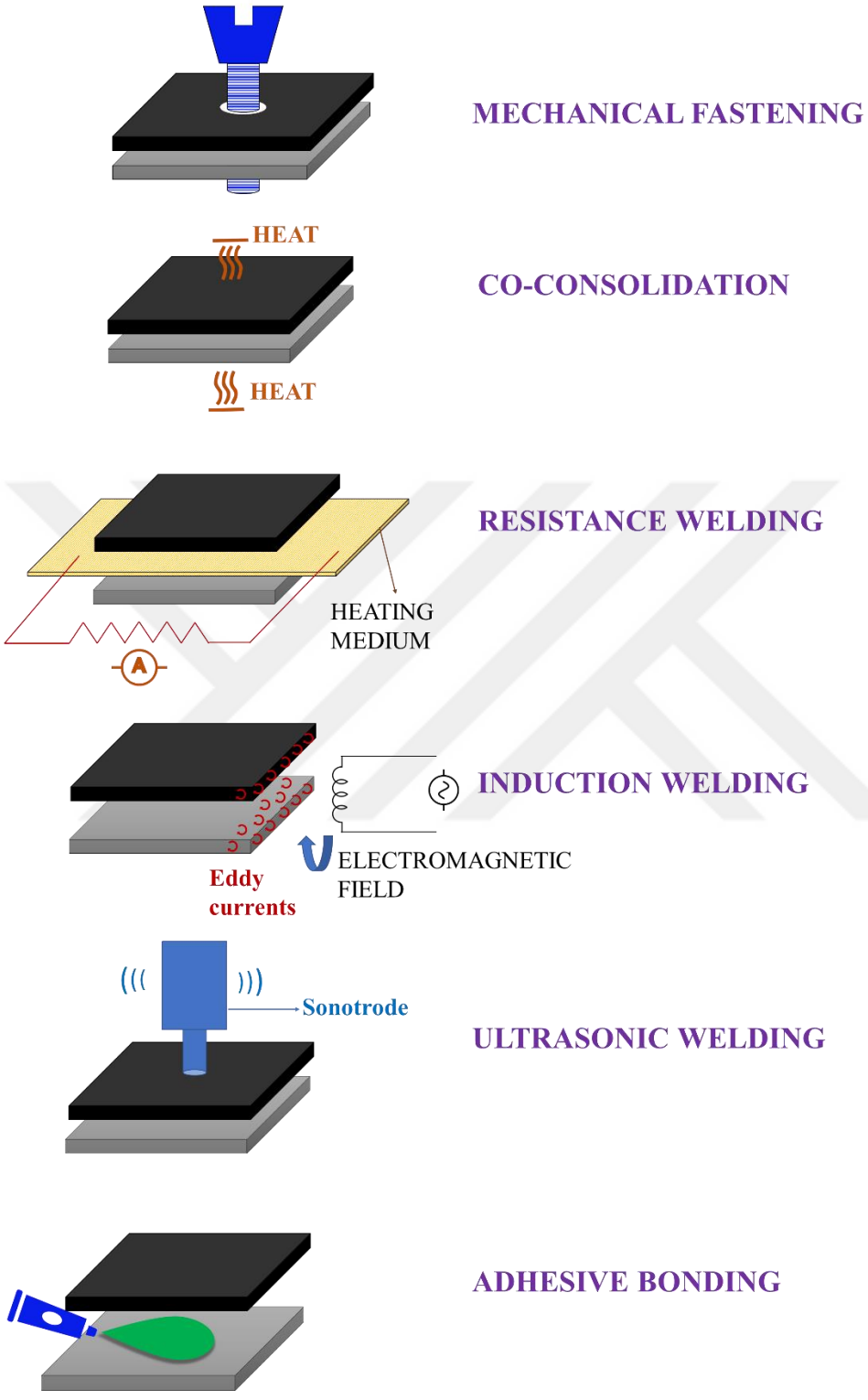

Figure 1.2 Schematics of the Joining Methods used for Thermoplastic Matrix Composite Structures all under Pressure.

(ii) ***Co-consolidation and Welding***

In this group, weak secondary bonds between the macromolecular chains of thermoplastic matrix are broken upon heating but they tend to re-bond again during pressing and cooling. The main problem in this group is the limitation in the size and geometry of two components to be joined. Because large and complicated shapes lead to difficulties in obtaining homogenous temperature distribution on their surfaces. Examples of the methods used in this group are:

- **Co-consolidation:** A heating source is used to provide heat to individual layers of consolidated laminates, and it softens the thermoplastic matrix to flow through the adjacent layers. Pressure is applied to intimate contact between the parts and promote intertwining of their molten polymer chains.
- **Resistance Welding:** A heating medium is used between consolidated laminates and current passes through it. As a result of sufficient current, heat is generated, and laminates under pressure are welded by intertwining of thermoplastic chains.
- **Induction Welding:** An external magnetic field is provided to form eddy currents on the composite surfaces. Hence, composite parts can be welded due to the interaction of macromolecular chains under pressure.
- **Ultrasonic Welding:** A sonotrode is used as the ultrasonic vibration source to heat the surfaces of the composite parts to be joined. Then, under pressure intertwining of the matrix chains would be possible.

(iii) ***Adhesive Bonding***

In this method, a kind of thermosetting polymer or oligomer is applied onto the surfaces to be joined, after pressing and curing reaction adhesion takes place. In the market, these adhesives are available in paste, bulk or film forms. “Paste adhesives” are two component systems (i.e. adhesive liquid resin and the curing agent), after mixing these two components, there would be a limited pot life to be applied. “Bulk

adhesives" are in the solid resin form, thus they require heating to get applicable viscosity. Both paste adhesives and bulk adhesives are especially preferred for repairment of cracked or damaged parts. On the other hand, for the joining of structural parts in aircraft industry, use of "Film Adhesives" are preferred. Thus, in this study, film adhesive form was used for joining of PPS/CF thermoplastic matrix composite laminate samples.

1.3 Joining by Using Film Adhesives

Film adhesives are generally partially cured thermosetting films laid in between the composite parts to be joined (Figure 1.3). Depending on the required joining performance one or more film adhesive layers could be used. In order to supply required heat energy and pressure for curing reaction properly joining of the parts are generally accomplished in an autoclave system. After proper curing, the main advantage of Film Adhesives compared to Paste Adhesives is the higher mechanical performance and uniform thickness throughout the joined surfaces.

It is stated that [1, 2] in aerospace industry, there are several advantages of using Film Adhesive joining technique compared to mechanical fastening, co-consolidation, and welding methods, such as;

- Continuous bonding along the assemble
- Reduced stress concentration sites
- Decrease in the weight of the component
- More uniform load distribution in the joint
- Reduced labor

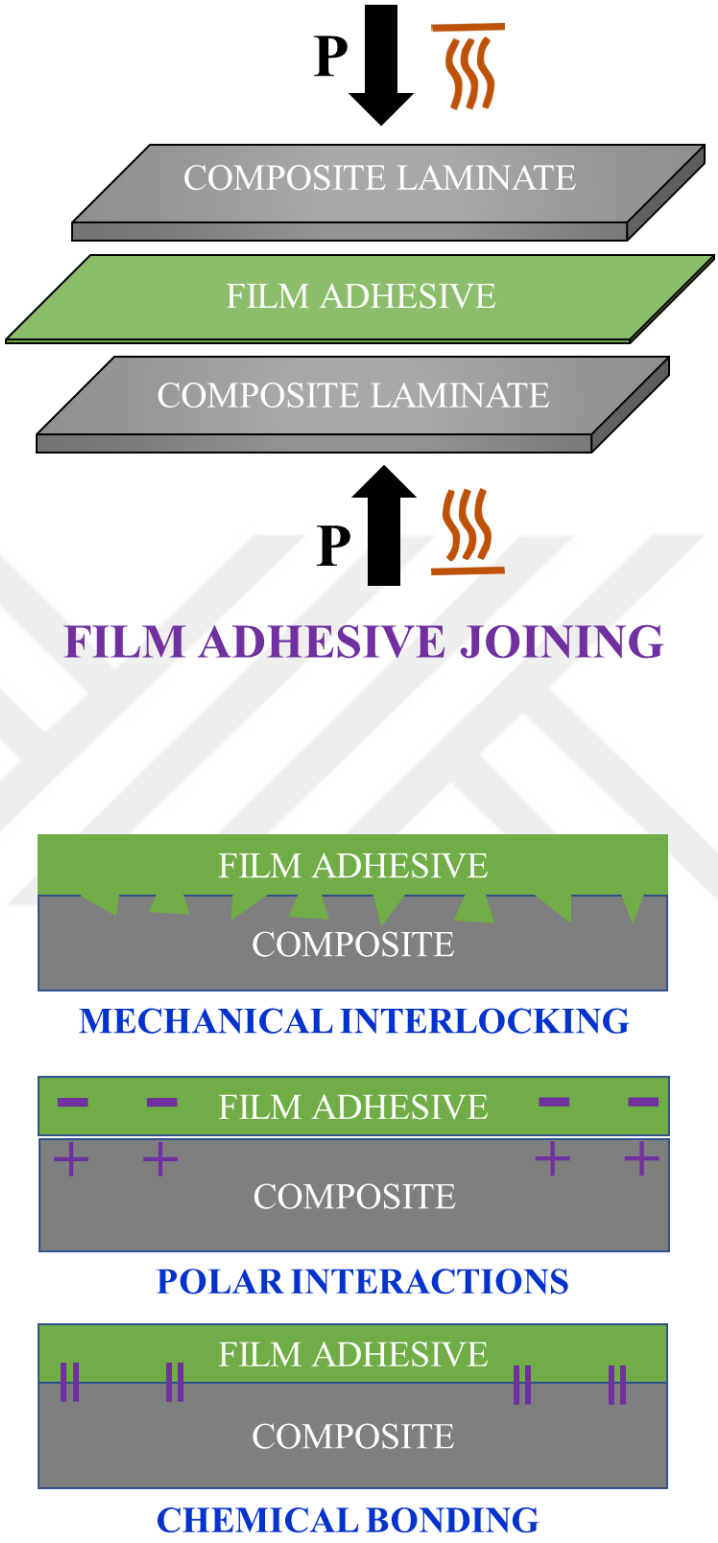

Figure 1.3 Schematics of the Film Adhesive Joining method and three Bonding Mechanisms that might occur.

As shown in Figure 1.3, during Film Adhesive Joining process, one or more well known bonding mechanisms could operate [3]. For instance, “Mechanical Bonding” might take place due to the certain degree of surface roughness leading to “interlocking” action at the interface. “Secondary Bonding” might occur due to the “polar interactions” between the surfaces. Of course, “Chemical Bonding” is the most significant mechanism due to the formation of primary covalent bonds at the interface.

In the aircraft industry, depending on the type of composite structures to be joined, different film adhesive materials are used. For instance, silicon based film adhesives are preferred for sealing applications such as window parts or door edges; acrylic based film adhesives for interior bins and lavatories; and polyurethane based film adhesives especially for the aircraft parts subjected to temperature variations. On the other hand, the most commonly used film adhesive materials are epoxy based ones due to their higher chemical resistance, higher mechanical performance and low shrinkage [4, 5]. Therefore, epoxy film adhesives are used to obtain durable joints in many structural critical parts of aircrafts, including wings and fuselage parts [6, 7].

1.4 Surface Treatments Used Before Film Adhesive Joining Method

It is known that since surface energies of the thermoplastic matrix composites are very low [8], surface characteristics of these parts to be joined play a very significant role in the effectiveness of Film Adhesive joining method. For instance, a degree of surface roughness might improve mechanical interlocking mechanism, while increased surface energies facilitate chemical bonding mechanism enormously. Therefore, in order to achieve proper Film Adhesive joining process, surfaces of these composite parts should be activated by using a kind of surface treatment technique.

For the thermoplastic matrix composite parts, available methods used in the aircraft industry can be categorized into two groups; “traditional mechanical treatments” such as “grit-blasting”, and “chemical energetic treatments” such as “plasma

treatment". In this study, effects of "grit-blasting" were compared with the results of "plasma treatment".

(i) ***Grit-blasting***

Grit-blasting is a mechanical process where the material surface is exposed to abrasive particles hitting the surface with high pressure. The impact of these particles causes surface textures leading to increase in roughness together with the removal of surface contamination. As shown in Figure 1.4, depending on the size and geometry of the composite parts to be joined, grit-blasting could be applied manually or in an automated system.

Grit-blasting leads to certain degree of cavities, i,e. surface roughness, to increase mechanical interlocking mechanism; while removal of surface contaminants might activate the functional groups present in the matrix polymer leading to improved chemical bonding mechanism [9]. On the other hand, improper use of grit-blasting might lead to certain problems, such as;

- Due to the accelerated particles, reinforcement fibers on the composite surface can be damaged.
- Treatment of large and complex shaped composite components could be very time-consuming.
- Since very high amount of particles are wasted, it would be very costly.
- Due to the very large amounts of dust generation, it would lead significant health issues for the workers, including the environmental problems.

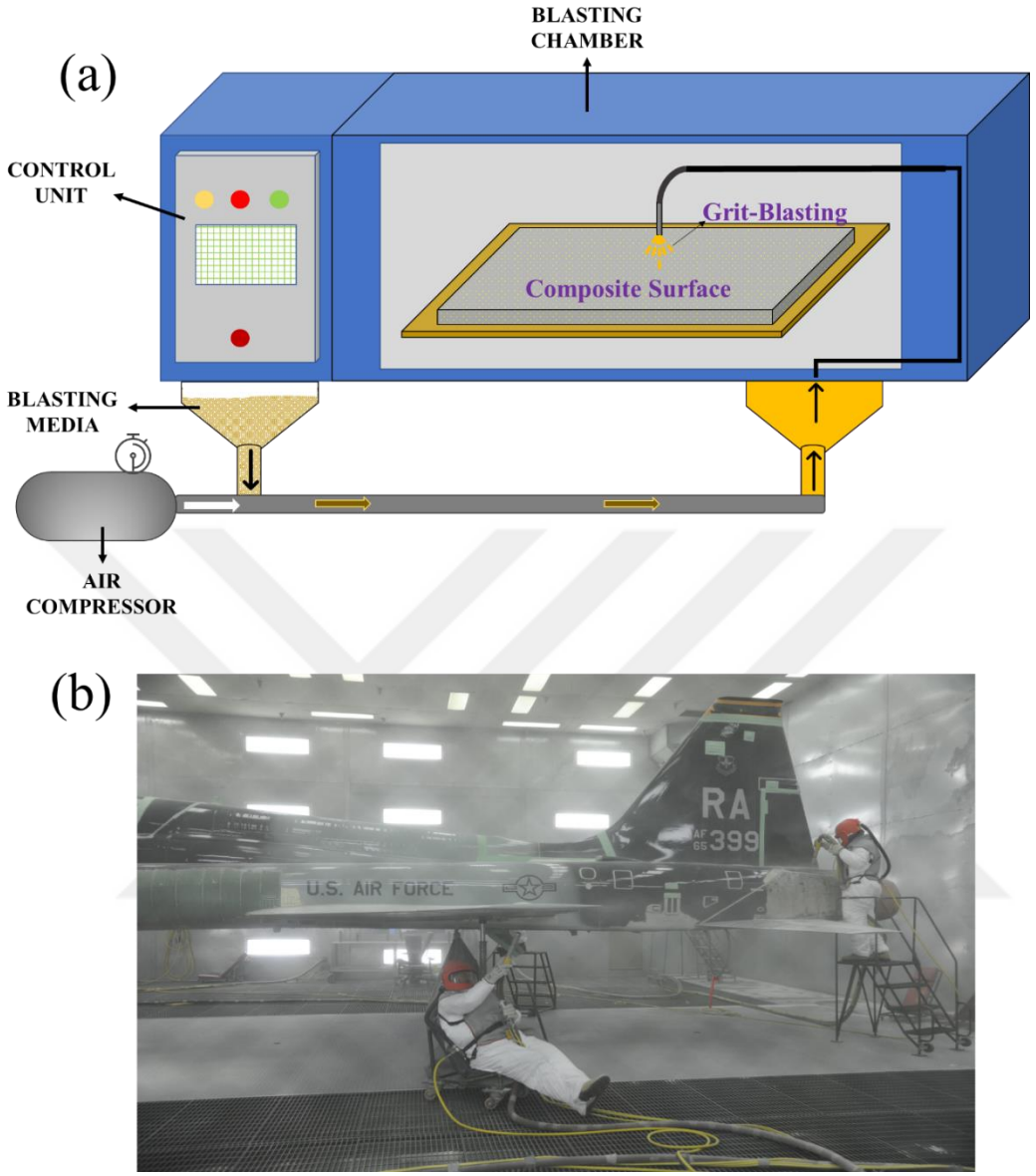

Figure 1.4 (a) Schematic of a typical Grit-blasting system, (b) manual application for large structures.

(ii) ***Atmospheric Plasma Treatment***

Plasma surface treatments are used for many polymer surfaces due to leading significant degree of surface activation required in many joining processes including film adhesive bonding [10]. Unlike the “low-pressure plasma” alternative under vacuum, atmospheric-pressure plasma systems, simply named as “atmospheric plasma”, provide in-line process capabilities, low prices, and minimal environmental and human safety requirements [11, 12].

In the atmospheric plasma systems, the inlet gas (oxygen, nitrogen, or air) is converted from gaseous state into plasma state upon exposure to very high voltage, then the jet is applied to the surfaces. As shown in Figure 1.5, main parameters during application of plasma jet onto the composite surfaces are the velocity of plasma jet and the distance between the nozzle and the surface.

For the thermoplastic matrix composites, since their surface energies are very low, plasma treatment reveals functional groups for the higher efficiency of chemical bonding mechanism required for high performance Film Adhesive joining.

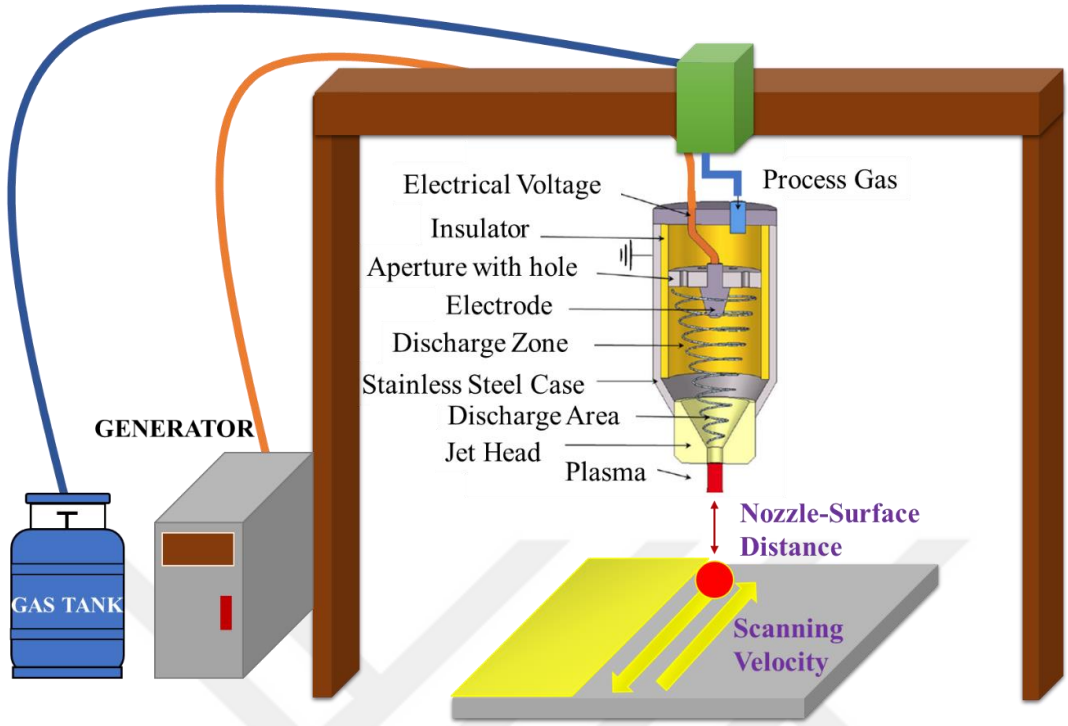

Figure 1.5 Schematic of the Atmospheric Plasma surface Treatment.

1.5 Literature Review

In the literature, it was observed that majority of the studies on the use of plasma surface treatment to improve joining performance of adhesive bonded composite structures were especially conducted for the traditional "thermoset matrix" composites [10, 13-26]. It was revealed that studies for the "thermoplastic matrix" composite structure were still very limited [27-34]; some of them [27-29] were conducted only for PP and PEEK matrices not for the PPS matrix; while some of them [30, 31] were conducted for joining of glass fiber (GF) reinforced PPS matrix composites onto Aluminium or Titanium metallic surfaces.

Thus, literature survey revealed that only three studies [32-34] were related to the effects of plasma surface treatment on the joining performance of adhesive bonded PPS/CF composite structures, as summarized below.

The first study by Blackman *et al.* [32] was conducted for the "unidirectional" Carbon Fiber reinforced PPS matrix composites joined by epoxy based "paste" and "film" adhesive forms. They indicated that, after applying oxygen plasma to the surfaces, due to the increase in the concentration of oxygen-containing polar groups, joining performance of the paste and film adhesive bonded specimens increased significantly. In terms of G_{IC} interlaminar fracture toughness energy, the increase was from 0.18 up to 1.45 kJ/m^2.

In the study of Iqbal *et al.* [33], effects of plasma treatment on joining performance were compared for the glass fiber (GF) and carbon fiber (CF) reinforced PPS matrix composites bonded with epoxy based paste adhesive. They indicated that due to the formation of functional groups and increased surface roughness after plasma treatment, joint performance of both PPS matrix samples improved. For instance, the increase in the single-lap shear strength values for the PPS/GF specimens was from 6 to 17 MPa, while for the PPS/CF specimens it was from 5 to 21 MPa.

In the recent study of Scarcelli *et al.* [34], PPS/CF composite surfaces were treated not only by plasma but also by ultraviolet radiation (UV) lamps for comparative purposes. Effects of these treatments on the joining performance of the PPS/CF samples were compered via epoxy based film adhesive. They pointed out that, due to higher increases in the surface free energies of the samples after plasma treatment compared to UV treatment, increase in the joint performance in terms of single-lap shear strength was from 3 MPa up to 24 MPa for the plasma treated ones, but it was up to 21 MPa for the UV treated samples.

1.6 Aim of the Thesis

As discussed above, literature review revealed that there were only three published works [32-34] investigating the effects of plasma surfaces treatment on the joining performance of PPS/CF composite parts bonded by film adhesive. Therefore, the main purpose of this thesis was to contribute this topic by conducting further experimental works with additional treatment parameters, testing and analyses.

For this purpose, after production of the PPS/CF composite laminates, their surfaces were plasma treated by changing two different parameters (plasma velocity and distance). Treated surfaces were characterized by various techniques including Contact Angle, Surface Energy, Surface Roughness, FTIR and XPS analyses. Then, joining performance of the PPS/CF composite samples bonded by an epoxy based film adhesive was determined by using three different mechanical tests; Single-lap shear strength, Mode-I interlaminar fracture toughness energy, and drop-weight impact toughness. Apart from “plasma” treated samples, all procedures were repeated also for the “untreated” and the conventional “grit-blasted” PPS/CF sample surfaces, for comparison.

CHAPTER 2

EXPERIMENTAL WORK

As discussed in the following sections, experimental work conducted in this study was basically composed of five steps; (i) production of PPS/CF thermoplastic composite laminates, (ii) plasma treatment of laminate surfaces, (iii) characterization of treated surfaces, (iv) joining of the samples by film adhesive bonding, and (v) mechanical testing to determine performance of the PPS/CF joints.

2.1 Production of PPS/CF Laminates to be Surface Treated and then Joined

As shown in Figure 2.1, production of the PPS/CF thermoplastic composite laminates to be surface treated and then joined were achieved in three main steps; (i) prepreg cutting, (ii) stacking and hot press consolidation of the prepregs, (iii) ultrasonic inspection and DSC analysis of the laminate samples. Details of these three steps were given below.

(i) *Cutting of PPS/CF Prepregs*

The commercial prepreg (*Toray-Tencate Cetex TC1100*) used in this study has polyphenylene sulfide (PPS) partially crystalline engineering thermoplastic matrix reinforced with continuous woven carbon fibers (CF) in 5-harness satin weave. As reported by the supplier, PPS matrix has glass transition temperature (T_g), melting temperature (T_m), and processing temperature (T_p) range of 90°C, 280°C, and 300-330°C, respectively. It was also stated that prepregs have 43 wt % resin content, 281 g/m^2 areal weight, and 0.31 mm ply thickness. As the first step, these prepreg layers were cut (Figure 2.1 (a)) from their roll by using an automated ply cutter.

(ii) ***Consolidation of PPS/CF Prepregs by Hot Pressing***

Laminates of PPS/CF were produced by stacking and consolidation of the cut prepreg layers via hot press compression molding method. In order to obtain 1.5 mm thick laminates, 5 plies were stacked on a hot plate surface covered by polyimide (*Kapton*) release film. Consolidation of the layers were achieved under a hot pressing system (*Langzauner Perfect*) (Figure 2.1 (b)) by applying three main processing parameters (Temperature, Pressure, Time) of 315°C, 550 kN, 10 minutes, respectively. After cooling, PPS/CF laminates produced (Figure 2.1 (c)) were ready for further procedures.

(iii) ***Ultrasonic Inspection and Differential Scanning Calorimetry (DSC) Analysis of the PPS/CF Laminates***

Non-destructive ultrasonic inspection was carried out for all PPS/CF laminates in order to reveal whether there was formation of voids, delamination or other damages during consolidation. For this purpose, an Automated Ultrasonic Through Transmission (AUTT) inspection technique (*Tecnotom Taurus Twin 2.0*) was used (Figure 2.1 (d)) by properly qualified personnel.

It should be noted that ultrasonic inspection was used not only after the production of the laminates. As would be discussed later in further sections, ultrasonic inspection was also performed to evaluate joining quality of the film adhesive bonding, and also during damage analyses of the drop-weight impact toughness tests.

After ultrasonic inspection, these large size PPS/CF laminates were cut into certain sizes required for further procedures, tests and analyses. For this purpose, an industrial cutting system (*Diamond-3 3515 RS*) with a cooling unit was used (Figure 2.1 (e)). After cutting, all surfaces were cleaned by isopropyl alcohol.

Since PPS is a partially crystalline thermoplastic polymer, it was important to measure crystallinity amount forming during hot press consolidation process. Thus,

differential scanning calorimetry (DSC) *(TA Instruments, Q100)* (Figure 2.1 (f)) analysis was conducted to determine the degree of crystallinity of PPS matrix during consolidation via double cycle heating profile from room temperature to 350°C at a rate of 10°C/min under nitrogen flow by using the following equation;

$$X_c(\%) = \frac{\Delta H_m - \Delta H_{cc}}{w_{PPS}\ \Delta H_m^{\circ}} x\ 100$$

where X_c is the percent crystallinity, ΔH_m is the melting enthalpy, ΔH_{cc} is the enthalpy of cold crystallization, w_{PPS} is the weight fraction of PPS matrix which is 0.43, and ΔH_m° is the melting enthalpy of 100% crystalline PPS which is reported as 150.4 J/g [35].

It should be again noted that DSC analysis was used not only after laminate production by hot press consolidation. Since joining of the laminates via Film Adhesive was achieved in an autoclave system, then it was also important to use DSC analysis to determine and compare the degree of matrix crystallinity "after the joining" process.

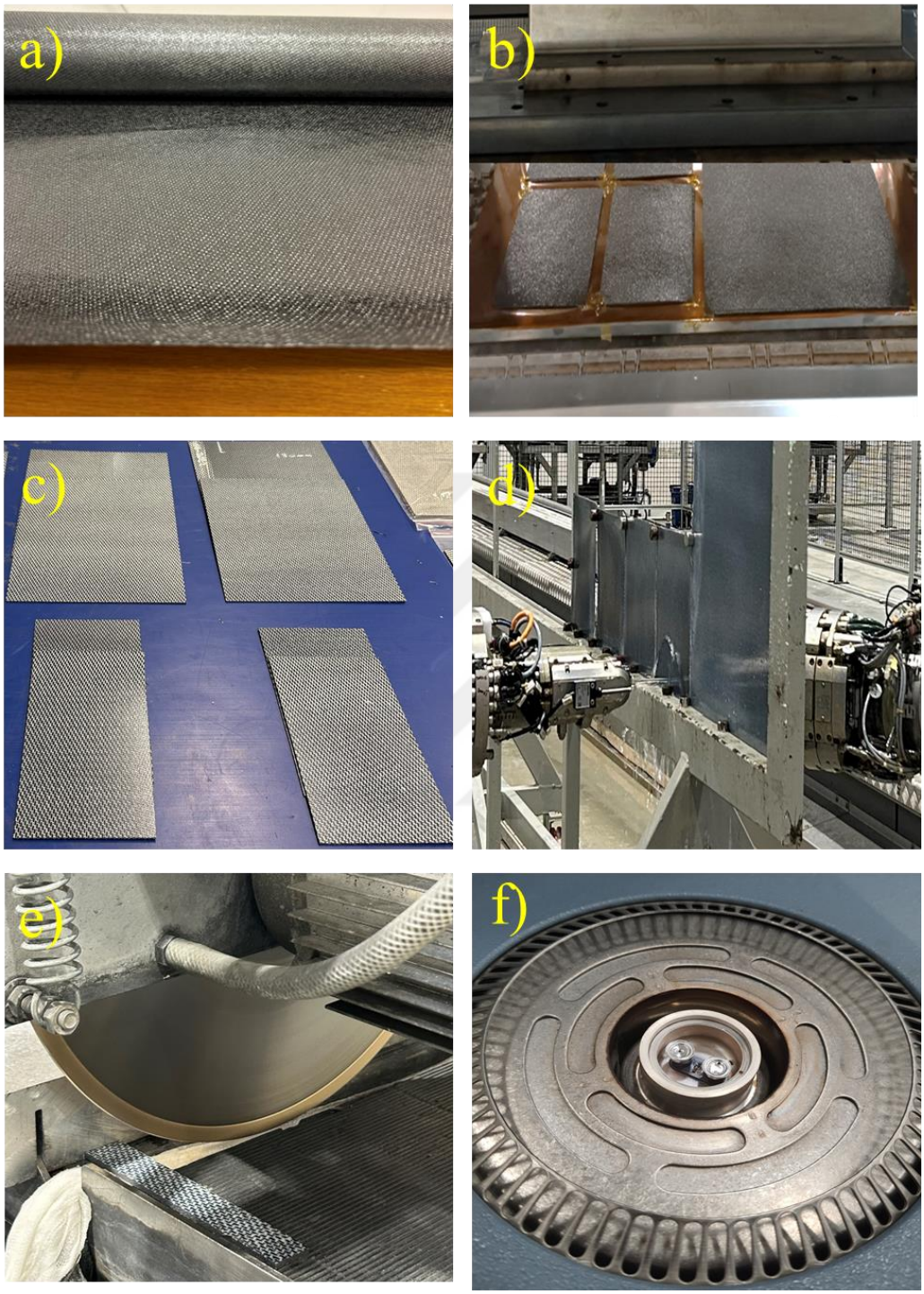

Figure 2.1 Steps during production of PPS/CF composite laminates; (a) cutting of one prepreg layer from the roll, (b) stacking and hot press consolidation of the five prepreg layers, (c) 1.5 mm thick laminates produced, (d) ultrasonic inspection of the produced laminates, (e) cutting of the laminates into certain sizes required, and (f) DSC analysis of the laminate samples.

2.2 Surface Treatments of PPS/CF Laminates Before Joining

In order to improve film adhesive joining of polymer matrix composite parts, their surfaces should be treated with a certain method to activate the bonding mechanisms at the interface. In this study, effects of "plasma" surface treatment were compared with the "untreated" and also with the traditional "grit-blasted" surfaces. These two surface treatments applied onto the PPS/CF laminates were explained below.

(i) *Grit-blasting*

Grit-blasting is a traditional surface treatment technique still used in the aircraft industry. In this method, grit (also named as sand) abrasive particles are accelerated by compressed air and blasted to the surface with controlled velocity and distance. As shown in Figure 2.2, PPS/CF laminate surfaces were blasted by aluminium oxide particles having average size of 177 μm (#80 mesh). Blasting was applied at an air pressure of 2.7 atm, through 8 mm diameter spray nozzle from a distance of 150 mm, and a projection angle of 45°-60° for 60 seconds. After grit-blasting, laminate surfaces were cleaned with water spray, and then dried in oven at 60° C for 2 hours.

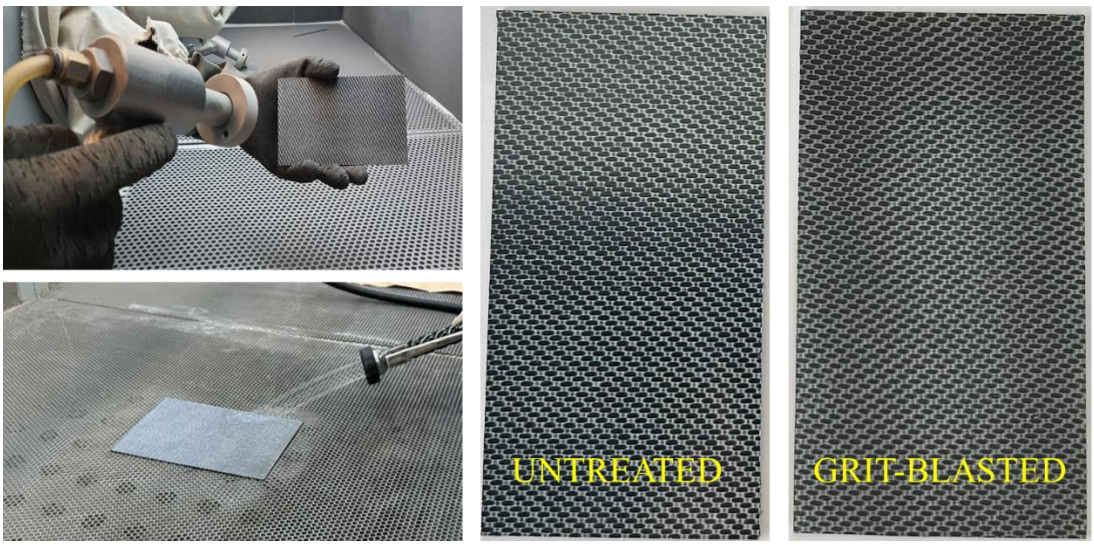

Figure 2.2 Grit-blasting and cleaning of PPS/CF laminate surfaces, and their appearance before and after the treatment.

(ii) ***Atmospheric Plasma Treatment***

Since plasma is the ionized gaseous state consisting of positively and negatively charged particles, use of plasma surface treatment is one of the most efficient technique to chemically activate the surfaces required for all adhesive bonding operations.

If the treatment system is operational under atmospheric-pressure, then it is called as "Atmospheric Plasma Treatment", which is much convenient compared to "low-pressure plasma" or "high-pressure plasma" techniques.

In this study, atmospheric-pressure plasma system used was *Plasmatreat GmbH* with a RD2004 model rotating plasma jet nozzle which could be connected to a robotic system (*TOYO, HKTM Robots*) to operate along x, y and z directions.

In this plasma treatment system (Figure 2.3), it was possible to use "air" as the plasma gas, on the other hand, "velocity" and "distance" of the plasma jet could be arranged. Therefore, in order to investigate effects of these two plasma parameters on the performance of film adhesive joining, the following three different values for each parameter were studied.

- **Velocity** of the Plasma Jet (mm/s): 10, 100, 200
- **Distance** between the Plasma Nozzle and Laminate Surface (mm): 11, 15, 20

After plasma treatments, surfaces of the laminates were protected by covering with aluminium foil (Figure 2.3), and the joining process was applied in a period not more than 3 hours.

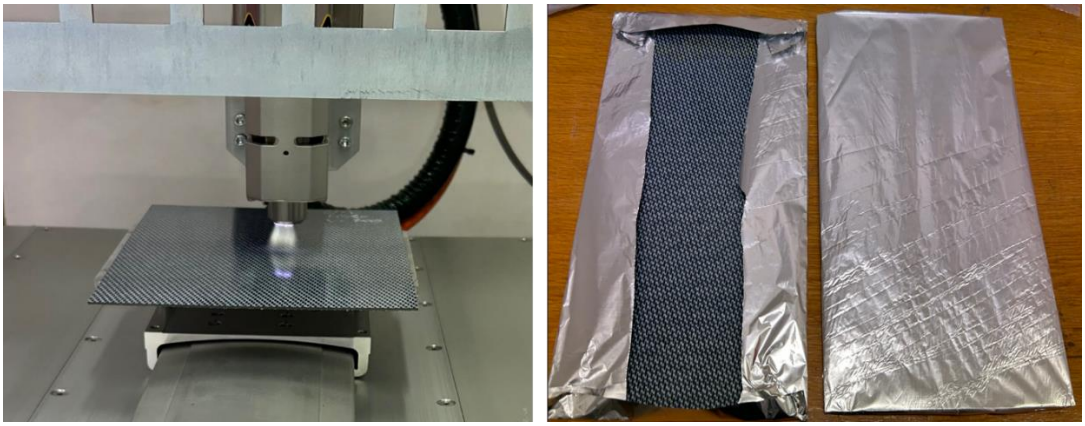

Figure 2.3 Atmospheric plasma surface treatment of PPS/CF laminates and protection of the treated surfaces until joining process.

2.3 Analyses of Surface Treated PPS/CF Laminates Before Joining

As explained below, in order to characterize untreated, grit-blasted and plasma treated PPS/CF laminate surfaces, four different analyses (Roughness, Wettability, FTIR, XPS) were conducted. Before them, Thermal Camera analysis was also conducted during the plasma treatment.

(i) *Thermal Camera Analysis*

That analysis during the plasma treatment was conducted in order to observe the degree and the distribution of the temperature on the surfaces of PPS/CF laminates, so that suitable combinations of "velocity" and "distance" parameters of the plasma jet could be selected.

For this purpose, temperature mapping of the PPS/CF surfaces during plasma treatment was recorded by *FLIR X6580sc* model thermal camera (Figure 2.4 (a)) placed approximately 1 meter away from the surface. Thermal emissivity value of PPS/CF surfaces required to obtain thermal mapping images was set as 0.90 as reported in the literature [36].

(ii) ***Surface Roughness Analysis***

Since surface roughness of PPS/CF laminates play a significant role especially on the mechanical bonding mechanism, surface topography of untreated and all treated 2x2 cm samples were examined under a contact type *MAHR* profilometer (Figure 2.4 (b)) stylus recording the vertical displacement as it moves. Then, surface roughness profile of the samples in accordance with ISO 16610-21 standard was obtained in terms of average roughness, R_a and R_z as the maximum height of the profile. For each sample surface, measurements were taken at least from 5 different regions.

(iii) ***Wettability Analysis (Contact Angle and Surface Free Energy)***

Effects of all surface treatments on the wettability were investigated first of all by contact angle measurements in accordance with ASTM D7334 standard via an optical tensiometer (*Biolin Scientific, Attention Theta Lite*) using 4-5 µL distilled water sessile droplets from 5 different regions ((Figure 2.4 (c)). Angle between the laminate surface and the water droplet was recorded by the camera within 10 seconds. Then, the contact angle (θ) was determined as the average of images taken in that period (Figure 2.4 (d)).

In this study, surface free energies of untreated and all treated laminates were estimated in accordance with ASTM D7490 standard based on Owens-Wendt-Kaelble method. In this method, apart from distilled water, another liquid with known dispersion and polar surface energy components is necessary. For this purpose, diiodomethane was used. Then, using the known dispersive and polar components of both liquids and the contact angle measured, surface free energies could be estimated by the following equation;

$$\frac{(1+\cos\theta)\gamma_l}{2} = [(\gamma_l^d \gamma_s^d)^{\frac{1}{2}} + (\gamma_l^p \gamma_s^p)^{\frac{1}{2}}]$$

where;

θ = Average contact angle measured

γ_l= Total surface tension of the liquids, mJ/m^2

γ^d and γ^p = Dispersion and Polar components of the liquids and the solid, mJ/m^2

Total surface tensions (γ_l) of distilled water and diiodomethane used are 72.8 and 50.8 mJ/m^2, respectively. Polar components (γ_l^p) of distilled water and diiodomethane are 51.0 and 1.3 mJ/m^2 while their dispersive components (γ_l^d) are 21.8 and 49.5 mJ/m^2, respectively. Then, Total Surface Free Energy of the laminates (γ_s) could be obtained by $\gamma_s = \gamma_s^p + \gamma_s^d$.

(iv)*Fourier-transform Infrared Spectroscopy (FT-IR)*

Fourier-transform infrared spectroscopy was conducted using *Perkin-Elmer Spectrum One® Spectrometer* with a universal sampling accessory ATR stage having Diamond/ZnSe crystal (Figure 2.4 (e)). In the infrared spectrum range of 600-4000 cm^{-1}, all treated surfaces were evaluated by comparing with the untreated surface. After backgrounding, a total of 50 scans at 4 cm^{-1} resolution were averaged for each laminate surface.

(v) *X-ray Photoelectron Spectroscopy (XPS)*

Chemistry of the treated PPS/CF laminate surfaces were also examined under an X-ray photoelectron spectrometer (*Thermo Fisher Scientific, K-Alpha*) (Figure 2.4 (f)). Elemental compositions of the treated surfaces were compared with the untreated one. XPS scanning energy spectrum was processed using the least square fitting software and the C 1s, S 2p and O 1s fine spectra were fitted with peak separation. For the emission of photoelectrons with element-specific binding energies, surfaces were scanned under monochromatic Al-Kα radiation (1486.7 eV).

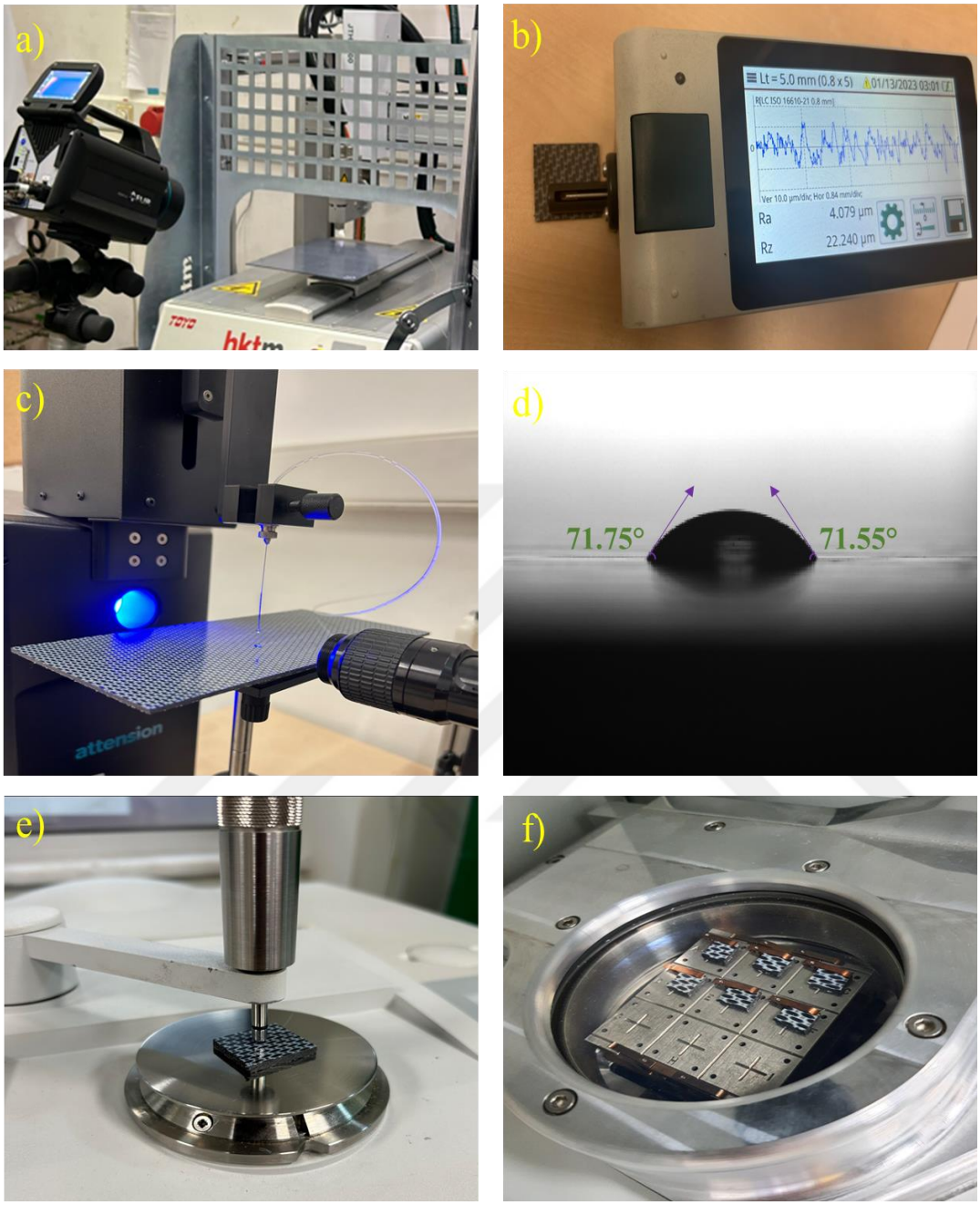

Figure 2.4 Analyses used to characterize untreated and treated PPS/CF laminate surfaces before joining; (a) Thermal Camera, (b) Surface Roughness, (c) and (d) Wettability-Contact Angle, (e) FTIR and (f) XPS.

2.4 Joining of PPS/CF Laminates with Film Adhesive Bonding

In this study, joining operations of untreated and all surface treated PPS/CF laminates were performed by using a commercially available epoxy-based Film Adhesive (*Solvay, Cytec FM 300K*) with a thickness of 0.2 mm and areal weight of 244 gsm. It is stated that shear strength of this aircraft industry purpose Film Adhesive at room temperature and 150°C are 35 MPa and 20 MPa, respectively. Due to its thermoset character, shelf-life of this green-colored adhesive film is given as 12 months if cold stored below -18°C.

Main steps used during Film Adhesive joining of PPS/CF laminate samples applied in clean room conditions are illustrated in Figure 2.5. First, green-colored film adhesive was peeled off from the upper and lower carrier films and cut into certain sizes suitable for the laminate samples (Figure 2.5 (a)); then, placed in between the two laminates to be joined (Figure 2.5 (b)).

Since the Film Adhesive material used was epoxy-based thermoset in the partially-cured flexible state, procedures applied during full-curing play a very significant role to achieve rigid and strong bonding in the joint. Therefore, for this purpose "vacuum bagging in the autoclave" approach was used as described below.

Laminates with Film Adhesive in between were placed on a tool and covered with a temperature resistant plastic bag (Figure 2.5 (c)) having vacuum connections to apply a vacuum pressure of 0.04 bar for compacting the layers. Then, three main full-curing parameters (i.e. Temperature= 180°C, Pressure= 3 bar, Time= 150 min) as advised by the Film Adhesive supplier were applied in an autoclave system (Figure 2.5 (d)).

After slow cooling (2-3°C/ min), Film Adhesive joined laminates were demoulded (Figure 2.5 (e)), and then cut into certain sizes for ultrasonic inspection, DSC analyses, and mechanical testing (Figure 2.5 (f)).

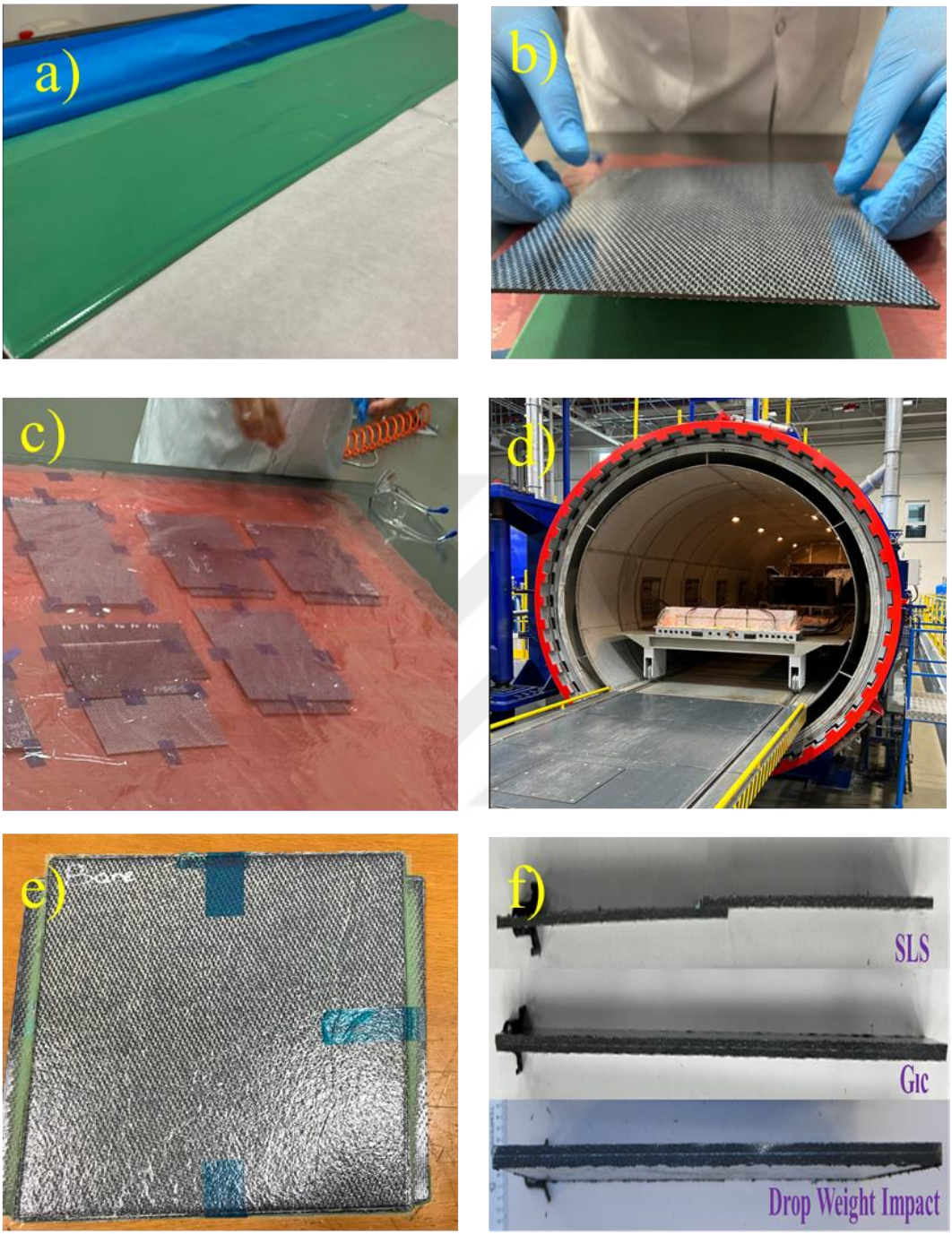

Figure 2.5 Joining of PPS/CF laminates with Film Adhesive; (a) Peeling-off the Film Adhesive from carrier films and cutting, (b) Placing the Film Adhesive in between the two laminates, (c) Plastic vacuum bagging, (d) Autoclave curing, (e) Laminate after joining, and (f) Mechanical test specimens extracted from joined laminates.

In order to compare effects of grit-blasting and plasma surface treatments applied to PPS/CF laminates on their joining performance bonded with Film Adhesive, the first technique used was non-destructive ultrasonic inspection of the joined laminates. For the determination of the partial crystallinity degree of PPS matrix, DSC analyses were also conducted. Then, mechanical performance of the joints were compared by conducting the mechanical tests described below.

2.5 Mechanical Testing of the Film Adhesive Joined Specimens

In order to evaluate joining performance of the untreated and all treated PPS/CF laminate samples, three different mechanical tests were conducted to determine and compare their "Interlaminar Shear Strength", "Interlaminar Fracture Toughness", and "Drop-Weight Impact Toughess" properties in accordance with the testing standards used for aerospace structures. Tests were conducted at laboratory conditions by using 250 kN capacity *Instron 5985 Universal Testing* system for SLSS and G_{IC} tests and *Instron-CEAST 9350 Drop Tower Impact* system for drop-weight impact test (Figure 2.6). For each specimen group four specimens were tested, and the properties were reported as average values with ± standard deviations.

(i) *Single Lap Shear Strength (SLSS) Tests*

This test was conducted in accordance with ASTM D5868 standard. Figure 2.6 (a) indicates the geometry and the interfacial joined area under shear supplied by tensile load. During the test, "Load versus Displacement" curves were recorded until the interlaminar shear failure occurred in the joined interface. Then, Single-Lap Shear Strength (SLSS) values were calculated by using the following relation:

$$SLSS = \frac{F_{max}}{l\ x\ w} x10^3 \qquad \text{(MPa)}$$

where;

F_{max}: Maximum load applied (kN)

l: Length of the joined area (12.5 mm)

w: Width of the joined area (25 mm)

(ii) ***Mode-I Interlaminar Fracture Toughness Energy (G_{IC}) Tests***

This test was conducted in accordance with the EN 6033 standard. The edge initial crack necessary was introduced by inserting a release film into the interface before the joining operations. Figure 2.6 (b) shows the geometry of the specimen and Mode-I loading (opening mode) fixture, where the total length of the specimen was 250 mm while initial crack length i.e. length of the release film was 25 mm. After obtaining "Load versus Displacement" curves when a total of 100 mm propagated crack length was reached, G_{IC} Fracture Toughness values were calculated by using the following relation:

$$G_{IC} = \frac{A}{a\ x\ w}\ x\ 10^6 \qquad \text{(J/m}^2\text{)}$$

where;

A: Area (J) under the load (N) versus displacement (m) curve for total crack growth.

a: Propagated crack length (100 mm)

w: Width of the specimen (25 mm)

(iii) ***Drop-Weight Impact Toughness Test***

The main purpose of this test conducted in accordance with ASTM D7136 standard is to evaluate resistance of the composite plate specimens against sudden impact loads. Impact Damage is imparted by a concentrated impact using a drop-weight with a hemispherical striker tip. In order to impart 50 Joules impact energy, the mass of

the impactor was 8.0 kg, while the diameter of hemispherical striker tip was 16mm. The impactor was dropped from a height of 635 mm onto the center of joined PPS/CF laminates having 150x100x4 mm plate dimension, which were placed firmly on the support fixture window frame of 125x75 mm (Figure 2.6 (c)).

Testing system (*Instron CEAST 9350*) records "Contact Force" versus Time data, which could be converted into "Absorbed Energy" versus Time curves. In this study, apart from evaluation of "maximum" values of Contact Force and Absorbed Energy (F_{max} and E_{max}), performance of the laminate specimens were evaluated also by examining the "dept" and "area" of the damages occurred. For this purpose, external damages were inspected by taking their top-view images under visible light and UV light qualitatively. Then, for the quantitative analyses, first of all, dept of the damages were measured with a digital depth indicator (*MarCator 1087 BR*). Then, for the through-thickness damage area determinations, Automated Ultrasonic Through Transmission (AUTT) inspections were conducted.

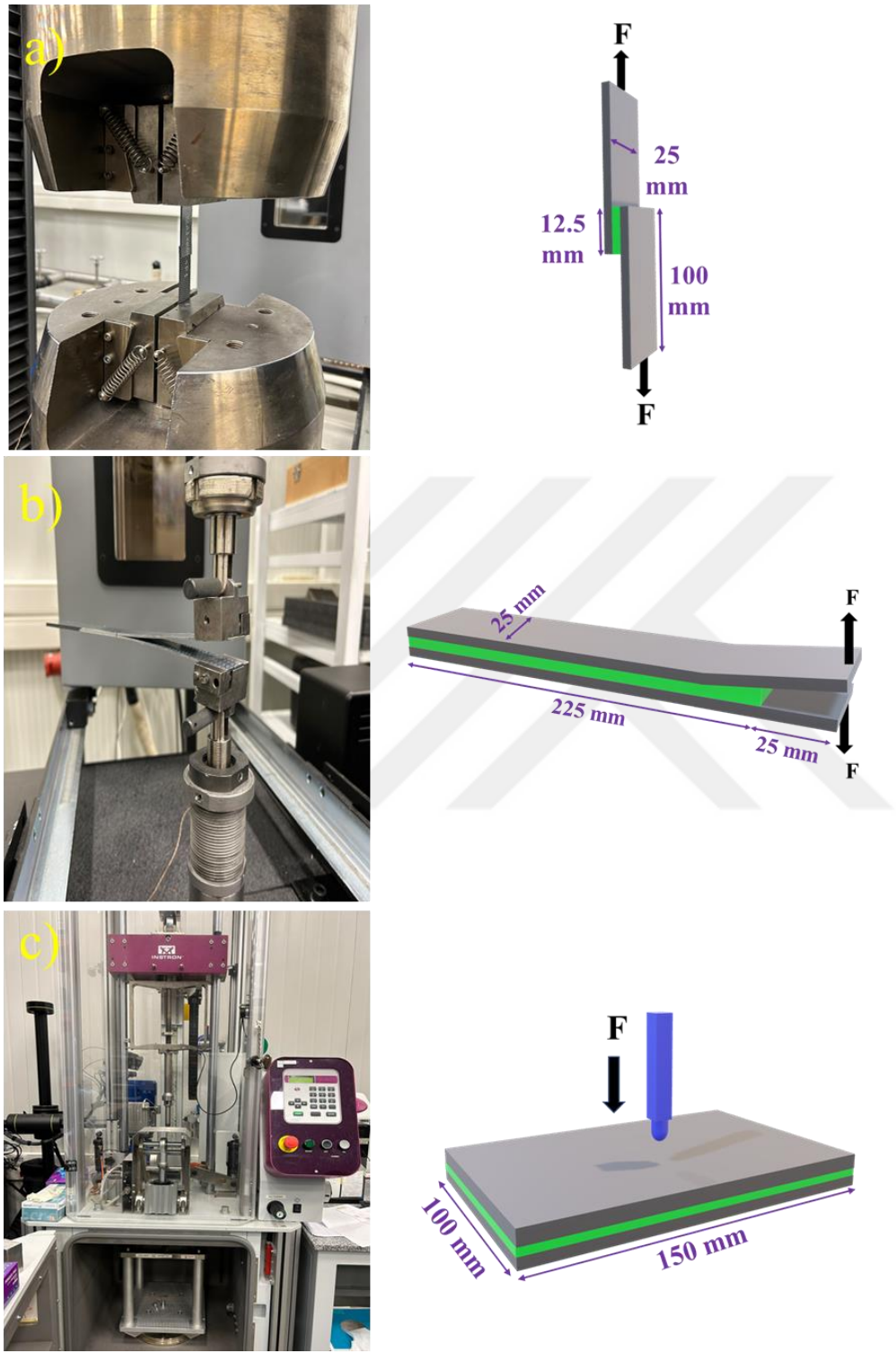

Figure 2.6 Loading fixture and specimen geometry of the mechanical tests used for joining performance; (a) Single-Lap Shear Strength, SLSS, (b) Mode-I Interlaminar Fracture Toughness, *GIc* and (c) Drop-Weight Impact Toughness.

CHAPTER 3

RESULTS AND DISCUSSION

The main purpose of this study was to observe the degree of the improvement on the Film Adhesive joining performance of PPS/CF thermoplastic composite laminates when their surfaces were treated by Atmospheric Plasma technique. For this purpose, plasma treated surfaces were compared with Untreated and the traditional Grit-blasted surfaces. In the following sections; first, selection of plasma treatment parameters were explained. Then, effects of Grit-blasting and Plasma treatments were compared in terms of changes on the roughness, wettability and chemistry of the surfaces. Finally, effects of all surface treatments on the joining performance were evaluated by applying three different mechanical tests.

3.1 Selection of Plasma Treatment Parameters by Thermal Camera Analysis

It is known that plasma surface treatment is a highly energetic technique leading to certain degree of heat energy developed on the surfaces of the samples. For the thermoplastic matrix composites, the temperature developed during plasma treatment should be much below the glass transition temperature (T_g) of the matrix polymer; which was around 88°C for PPS matrix. Thus, during trials for the selection of the plasma treatment parameters, thermal camera analysis was used.

In the plasma treatment system used, there were two parameters that can be changed; “Plasma Scanning Velocity” simply designated as “V”, and the “Plasma Nozzle-Surface Distance” simply designated as “D”. After several trials with thermal camera mapping, three values for each parameter were selected. That is, for the plasma scanning velocity V=10, 100, 200 mm/s; and for the plasma nozzle-surface distance D=11, 15, 20 mm. Their combination resulted in five different specimen type. As

shown in Table 3.1, these five different specimens were designated by using the format "Plz-V*xx*-D*yy*", where *xx* represents velocity value used in mm/s; while *yy* represents distance value used in mm.

As indicated in Figure 3.1, surface temperature values during plasma treatments were recorded for the hottest zone (i.e. center of the red colored zone in the temperature mapping) just beneath the nozzle. Then, average values of these temperatures recorded for each specimen type were tabulated in Table 3.1. It was seen that temperature of the surfaces slightly decreased with increasing plasma Velocity and Distance. The highest surface temperature developed during plasma treatments was 66°C (for Plz-V10-D11), while the lowest surface temperature developed was 56°C (for Plz-V200-D11). Since these temperatures developed were all well below the T_g of the PPS matrix, it could be stated that there would be no thermal detrimental effect of plasma treatment parameters selected.

Table 3.1 Specimen Designation and values of the Plasma Velocity and Plasma Distance parameters selected for each one; and average values of the Surface Temperatures recorded by Thermal Camera.

Specimen Designation	**Plasma Velocity, V (mm/s)**	**Plasma Distance, D (mm)**	**Surface Temperature (°C)**
Plz-V10-D11	10	11	66.1 ± 0.2
Plz-V10-D15	10	15	64.9 ± 0.2
Plz-V10-D20	10	20	58.6 ± 0.2
Plz-V100-D11	100	11	65.0 ± 0.1
Plz-V200-D11	200	11	56.1 ± 0.1

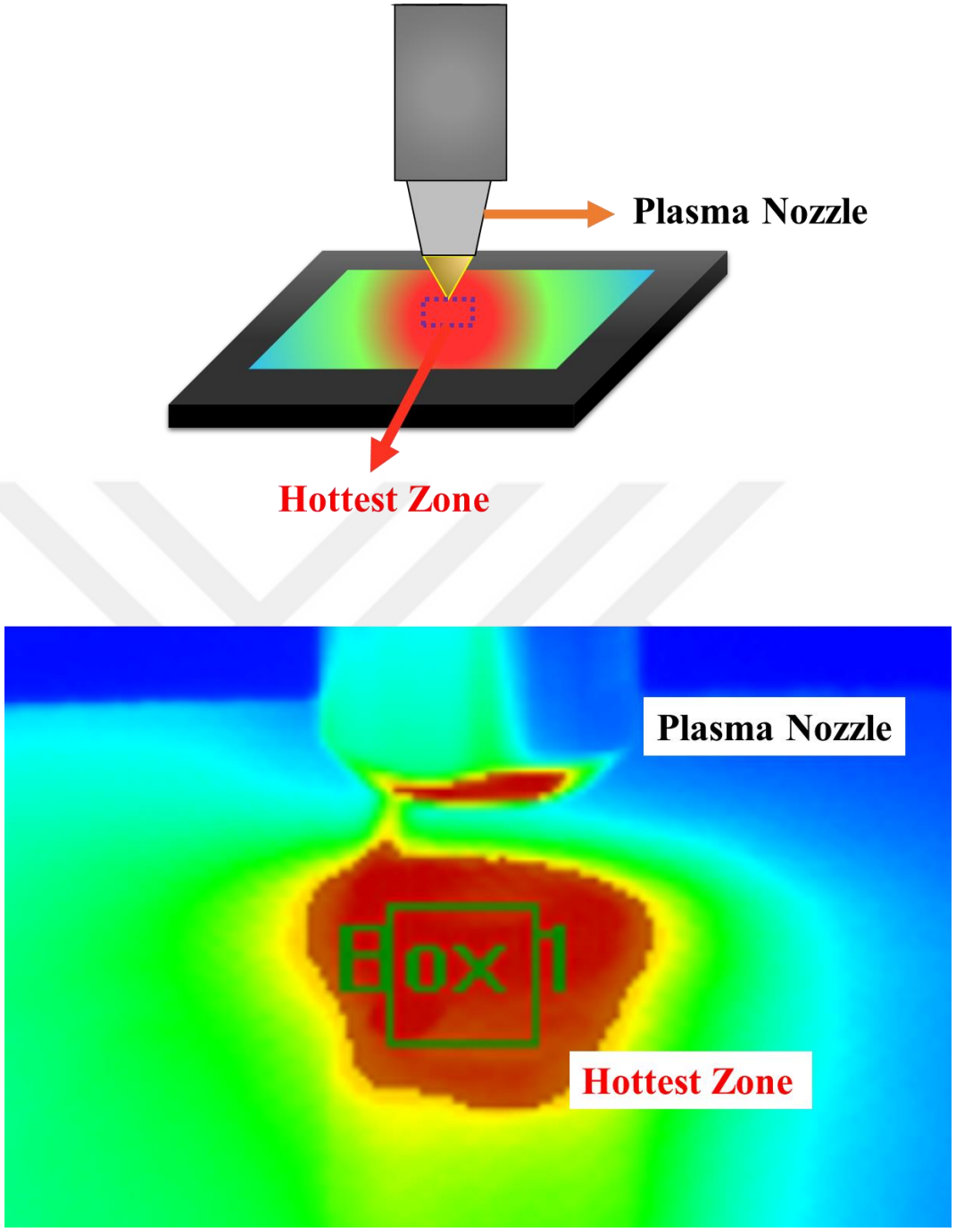

Figure 3.1 Schematics of Thermal Camera analysis, and an example of temperature mapping image obtained during plasma treatment of PPS/CF surfaces.

3.2 Changes in the Roughness of Treated PPS/CF Surfaces

For all types of joining techniques, surface texture in terms of surface roughness become a critical parameter for the "interlocking mechanism" also defined as "mechanical bonding" at the interface. Therefore, in order to reveal the degree of mechanical bonding mechanism, surface roughness measurements of Untreated, Grit-blasted and all Plasma treated specimens were performed by using contact type profilometer. Average values of the surface roughness in terms of both *Ra* and *Rz* for all specimens were tabulated in Table 3.2, and the values were compared in Figure 3.2

It was seen that after Grit-blasting, surface roughness values of the Untreated surface increased enormously, the increase in *Ra* being from 0.45 up to 3.57 μm, while in *Rz* from 2.38 up to 21.0 μm; that is, increases were more than 7 times and 8 times, respectively. Thus, as would be discussed later, the dominant bonding mechanism in the Film Adhesive joining of Grit-blasted PPS/CF laminates were proposed as mechanical interlocking mechanism.

On the other hand, after Plasma treatments, increases in the *Ra* and *Rz* surface roughness values were limited, e.g. for the Plz-V10-D11 specimen, these increases were only 22% and 19%, respectively; i.e. from 0.45 to 0.55 μm for *Ra*, and from 2.38 to 2.83 μm for *Rz*. Table 3.2 and Figure 3.2 also indicated that increasing the plasma Velocity and plasma Distance parameters resulted in further slight decreases in the *Ra* and *Rz* surface roughness values; the lowest values being 0.47 μm for *Ra* and 2.34 μm for *Rz*. Thus, as would be discussed later, the dominant mechanism in the Film Adhesive joining of Plasma treated PPS/CF laminates were proposed as chemical interactions between the surfaces.

It was stated in the literature [37-41] that the main reason for the slight increases or decreases on the surface roughness values during plasma treatments was the physical and energetic interactions between the positively and negatively charged ionized plasma particles and the atoms or molecules present at the surface.

Table 3.2 Average Surface Roughness values in terms of *Ra* and *Rz* for the Untreated and treated PPS/CF surfaces.

	Ra **(µm)**	***Rz*** **(µm)**
Untreated	0.45 ± 0.06	2.38 ± 0.26
Grit-blasted	3.57 ± 0.12	21.0 ± 0.79
Plz-V10-D11	0.55 ± 0.07	2.83 ± 0.43
Plz-V10-D15	0.55 ± 0.08	2.71 ± 0.46
Plz-V10-D20	0.52 ± 0.04	2.68 ± 0.23
Plz-V100-D11	0.51 ± 0.05	2.56 ± 0.19
Plz-V200-D11	0.47 ± 0.05	2.34 ± 0.28

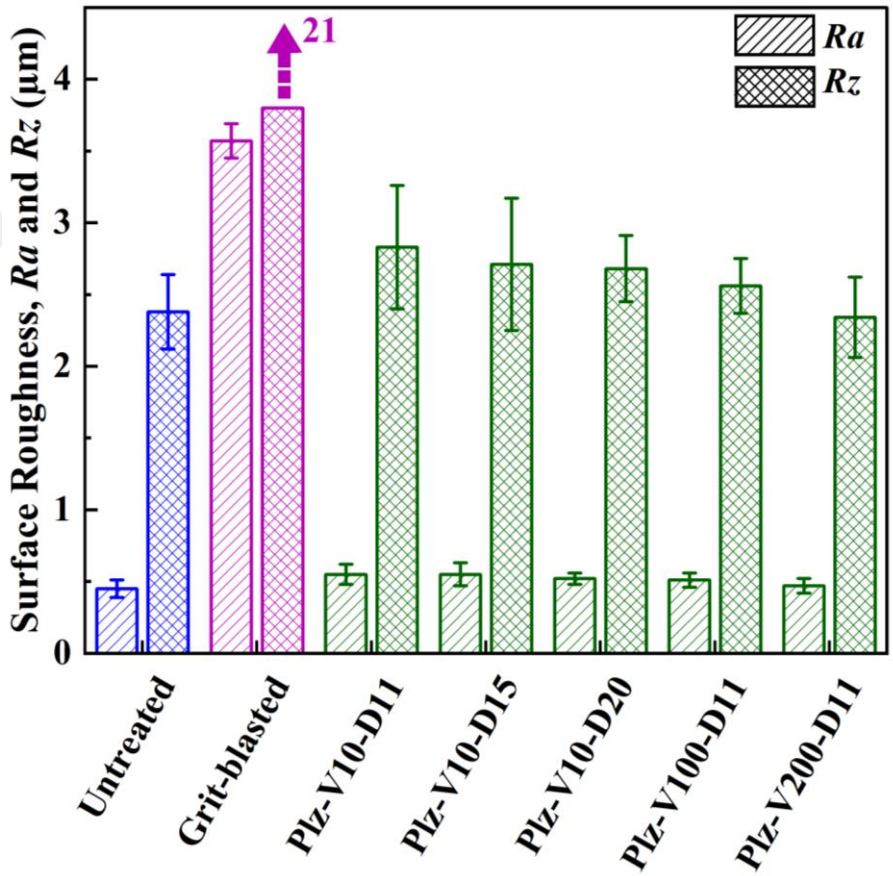

Figure 3.2 Effects of Grit-blasting and Plasma Treatments on the Surface Roughness (*Ra* and *Rz*) of PPS/CF specimens.

3.3 Changes in the Wettability of Treated PPS/CF Surfaces

For any kind of Adhesive Bonding during joining of composite parts, the first requirement is to have certain degree of “wettability” of adhesive medium on the surfaces of the parts to be joined; which is also valid for the Film Adhesive joining of PPS/CF composite laminates. Therefore, in order to reveal the degree of wettability, “Contact Angle” measurements and “Surface Free Energy” estimations were performed for Untreated, Grit-blasted, and all Plasma treated specimens as described before. Average values of “Water Contact Angle” and “Total Surface Free Energy” including its “Polar” and “Dispersion” components were tabulated in Table 3.3, and the values were compared in Figure 3.3.

(i) *Contact Angle*

It is known that decreasing the Contact Angle values increases the spontaneous wetting condition of the surfaces. Table 3.3 indicated that after Grit-blasting, Water Contact Angle value of Untreated surface increased slightly from 72.5° to 78.6°. As discussed in the literature [42-44], the reason of these unwanted increases was basically due to the very high level of surfaces roughness topography with so many numbers of high peaks and narrow valleys preventing the water droplets from penetrating into these extensive degree of surface irregularities.

On the other hand, after all Plasma treatments, it was seen that there was enormous decrease in the Water Contact Angle value of the Untreated surface. For instance, the decrease for the Plz-V10-D11 specimen surface was from 72.5° down to 12.8°, i.e. a decrease of more than 5 times. For the Plz-V200-D11 specimen surface, Water Contact Angle was 29.8°, this time a decrease of more than 2 times.

(ii) ***Surface Energy***

For the efficient Film Adhesive joining method, apart from lower Contact Angle values, Surface Free Energy of the surfaces should be as high as possible. It was seen in Table 3.3 that Total Surface Free Energy of the Untreated specimen increased only 8% (i.e. from 46.8 to 50.9 mJ/m^2) for the Grit-blasted specimen. Contrarily, after all Plasma treatments very significant increases were observed, e.g. for Plz-V10-D11 specimen the increase was 57% (up to 73.8 mJ/m^2), while for Plz-V200-D11 specimen it was 42% (up to 66.7 mJ/m^2).

Of course, as also pointed out in the literature [45, 46], for the joining performance of all Adhesive Bonding methods, "Polar component" of the Surface Free Energy plays a much more significant role. Table 3.3 revealed that for the Untreated and Grit-blasted surfaces Polar components were extremely low being only 6.0 and 2.5 mJ/m^2, respectively. Plasma treatments increased Polar component significantly being all above 32 mJ/m^2. This could be interpreted that plasma surface treatments applied might lead to certain polar interactions and chemical bonding mechanism between the Film Adhesive and PPS/CF surfaces.

Table 3.3 Average values of the Water Contact Angle and Total Surface Free Energy including its Polar and Dispersion Components of Untreated and Treated PPS/CF surfaces.

	θ **Water Contact Angle (°)**	γ_s **Total Surface Free Energy (mJ/m^2)**	γ_s^p **Polar Component (mJ/m^2)**	γ_s^d **Dispersion Component (mJ/m^2)**
Untreated	72.48 ± 1.18	46.85 ± 1.47	6.02 ± 0.16	40.83 ± 1.30
Grit-Blasted	78.63 ± 3.09	50.91 ± 0.23	2.47 ± 0.93	48.44 ± 0.71
Plz-V10-D11	12.85 ± 1.29	73.84 ± 0.68	37.54 ± 0.42	36.30 ± 1.11
Plz-V10-D15	16.41 ± 0.28	72.83 ± 0.47	36.67 ± 0.75	36.16 ± 1.21
Plz-V10-D20	18.34 ± 2.69	72.03 ± 0.65	36.29 ± 1.47	35.74 ± 0.83
Plz-V100-D11	26.67 ± 2.36	68.84 ± 1.64	32.77 ± 1.24	36.06 ± 2.22
Plz-V200-D11	29.81 ± 2.88	66.75 ± 1.94	32.17 ± 0.68	35.58 ± 1.27

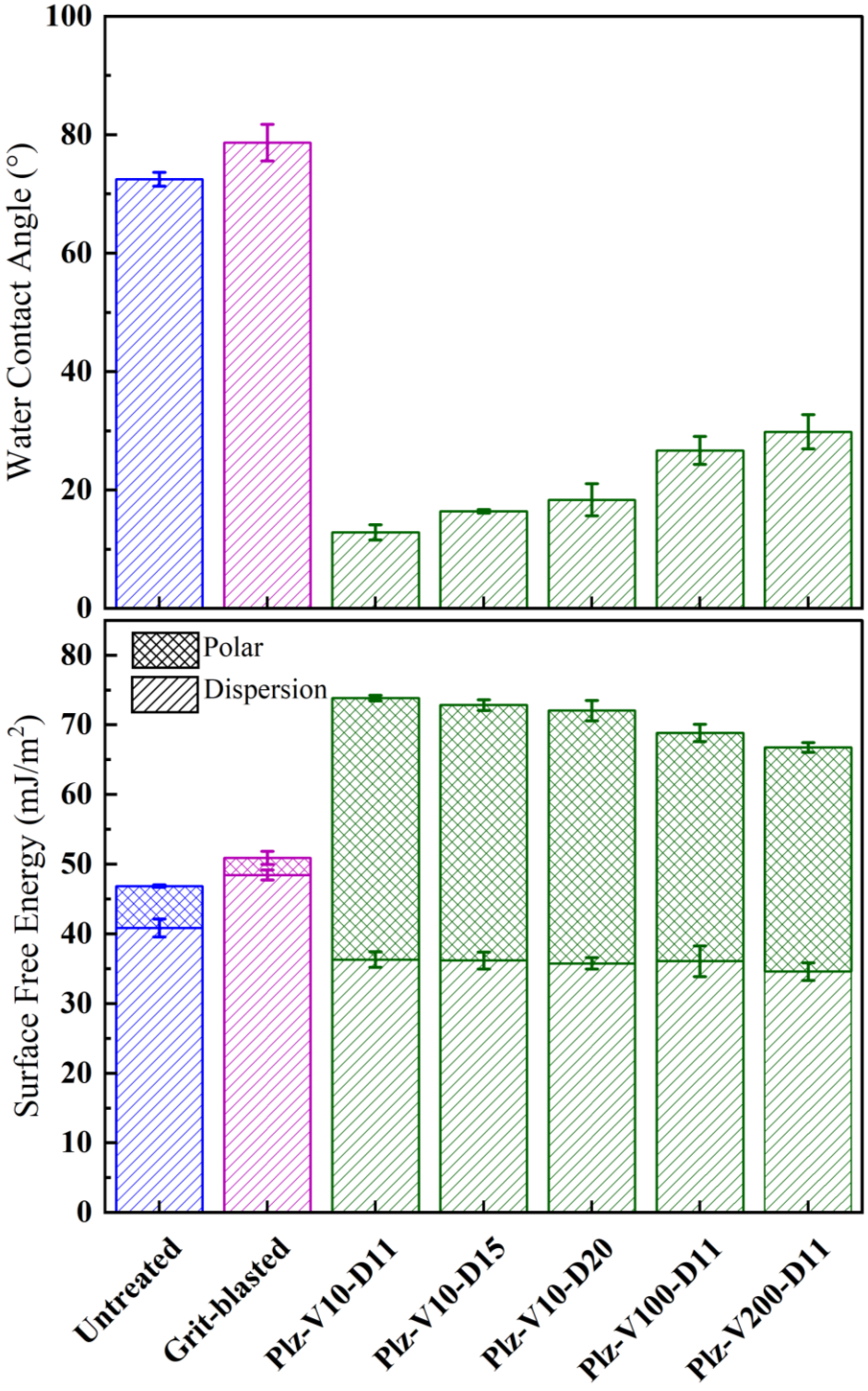

Figure 3.3 Effects of Grit-Blasting and Plasma Treatments on the Water Contact Angle and Total Surface Free Energy including its Polar and Dispersion Components of PPS/CF surfaces.

3.4 Changes in the Chemistry of Treated PPS/CF Surfaces

It is known that joining performance of all Adhesive Bonding methods could be improved by increasing polar interactions and chemical bonding mechanisms at the interface. Therefore, in order to observe changes in the chemistry of all treated PPS/CF surfaces compared to the Untreated one, two different but complementary chemical analyses were conducted: Fourier Transform Infrared Spectroscopy (FTIR) and X- ray Photoelectron Spectroscopy (XPS).

(i) *FTIR*

For comparison, FTIR spectra obtained for the Untreated, Grit-blasted and one of the Plasma treated (Plz-V10-D11) surfaces were illustrated in Figure 3.4. The first spectrum in this figure was for the Untreated sample, thus all the characteristic IR peaks attributed for PPS matrix polymer cited in the literature [47, 48] were observed. That is, peaks at 1573, 1470, and 1384 cm^{-1} for the stretching vibration of C-C bonds, while 1008 cm^{-1} for the stretching vibration peak of C=CH in benzene ring. The peak at 1094 cm^{-1} is attributed to the stretching vibration of the C-S bond and 803 cm^{-1} corresponds to vibration peak of C-H in benzene ring.

Since Grit-blasting is rather a mechanical surface treatment changing mainly surface roughness topography, Figure 3.4 indicated that there were no apparent differences between the spectrum of Untreated surface and the spectrum of Grit-blasted surface.

On the other hand, Figure 3.4 revealed that there were certain new IR peaks formed after Plasma treatment, such as functional O-H peaks at 3364 cm^{-1}, carbonyl C=O stretching at 1643 cm^{-1}, vibration of C-O at 1286 cm^{-1}, stretching vibrations of -SO_2- at 1200 cm^{-1}, and S=O at 1074 cm^{-1}. In the literature [49-51], it was discussed that appearance of these new IR peaks could be due to the oxidative action of the plasma treatment on the PPS polymer structure.

When plasma Velocity and Distance were increased, it was observed that there were no significant changes in their IR spectra compared to Plz-V10-D11 sample, only intensities of these new peaks were decreased. Thus, it could be pointed out that, formation of these chemically reactive sites (OH, C=O, C-O, -SO_2-, S=O) after plasma treatments would improve chemical Adhesive Bonding mechanism of PPS/CF samples.

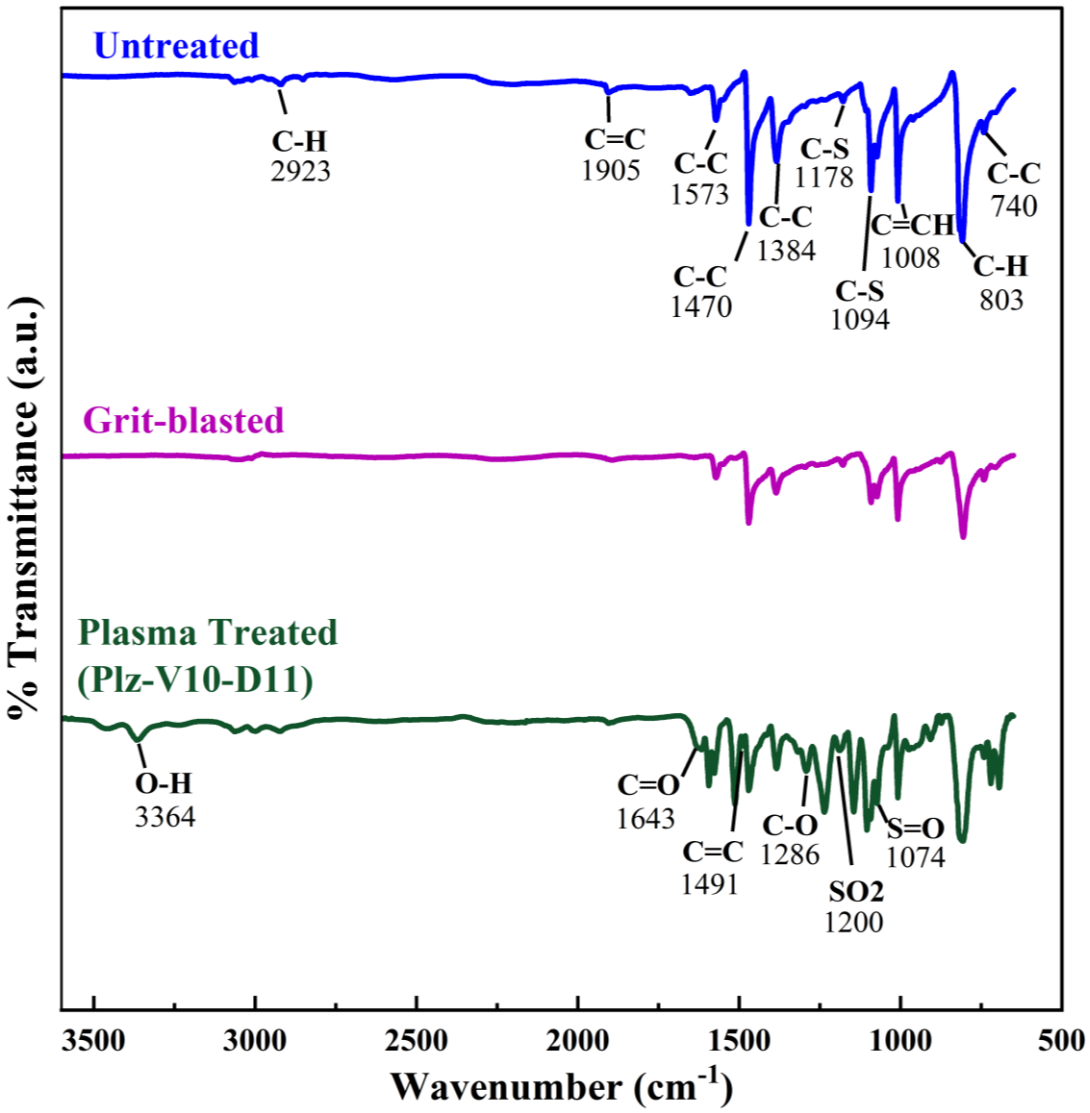

Figure 3.4 FT-IR spectra of the Untreated, Grit-Blasted and one of the Plasma Treated (Plz-V10-D11) PPS/CF surfaces.

(ii) *XPS*

In Figure 3.5, XPS spectra obtained for the Untreated, Grit-blasted and one of the Plasma treated (Plz-V10-D11) surfaces were given. It was seen that spectrum of Untreated and Grit-blasted surfaces were composed of three main elements; carbon (C1 s) at 285.1 eV, Sulphur (S 2p) at 164.1 eV, and oxygen (O 1s) at 532.1 eV. Due to the ionized nitrogen species in the air plasma, a tiny peak for nitrogen (N 1s) at 402.1 eV was also appeared for the Plasma treated surfaces.

In order to compare changes in the chemistry of Grit-blasted and Plasma treated surfaces, elemental compositions in atomic percentages were tabulated in Table 3.4 as the average of the measurements taken from the resin-rich and fiber-rich regions. Additionally, to reveal oxidation level of two main elements carbon and sulphur present in PPS matrix polymer, O/C and O/S atomic ratios were also determined and tabulated.

Table 3.4 indicated that increases in the O/C atomic ratio of Untreated surface were from 0.059 to 0.153 after Grit-blasting, while it was up to 0.693 after Plz-V10-D11 plasma treatment. Similarly, increases for the O/S atomic ratio was from 0.378 to 1.527 for Grit-blasting, while it was up to 3.054 for the Plz-V10-D11 surfaces.

These very significant increases in the O/C and O/S atomic ratios after Plasma treatments could be interpreted that both C and S elements in the PPS matrix polymer were oxidized considerably. Of course, increasing plasma Velocity and Distance resulted in slight decreases in these atomic ratios.

In Figure 3.6, in order to reveal these oxidized polar groups on the surfaces of Plz-V10-D11 Plasma treated sample, main peaks of C 1s and S 2p were deconvoluted and compared with C 1s and S 2p peaks of Untreated surface. It was seen that three new peaks under C 1s envelope appeared which represent formation of the oxidation bonds of C-O at 286.7 eV, C=O at 288.7 eV and O=C-O at 291.3 eV. Likewise, three new peaks were observed under S 2p envelope, indicating the oxidation bonds of

S=O at 166.4 eV, O=S=O at 167.4 eV and SO2-OH at 169.9 eV. Similar observations were also cited in the literature [52, 53].

Thus, it could be again stated that, formation of these polar groups, such as C=O, O=C-O and S=O, after plasma treatments would improve Film Adhesive joining performance of PPS/CF laminate surfaces.

Table 3.4 XPS Elemental Compositions (C, O, S, N) including O/C and O/S Atomic Ratios of the Untreated, Grit-blasted and Plasma Treated PPS/CF Surfaces.

	C (at %)	**O (at %)**	**S (at %)**	**N (at %)**	**O/C**	**O/S**
Untreated	81.1	4.80	12.9	1.1	0.059	0.378
Grit-Blasted	76.4	11.5	7.50	2.0	0.153	1.527
Plz-V10-D11	48.8	33.4	10.9	5.7	0.693	3.054
Plz-V10-D15	52.1	30.1	10.8	5.6	0.578	2.767
Plz-V10-D20	66.0	20.7	9.20	2.2	0.313	2.241
Plz-V100-D11	65.8	20.3	9.70	2.4	0.309	2.106
Plz-V200-D11	77.8	11.8	6.90	2.1	0.152	1.730

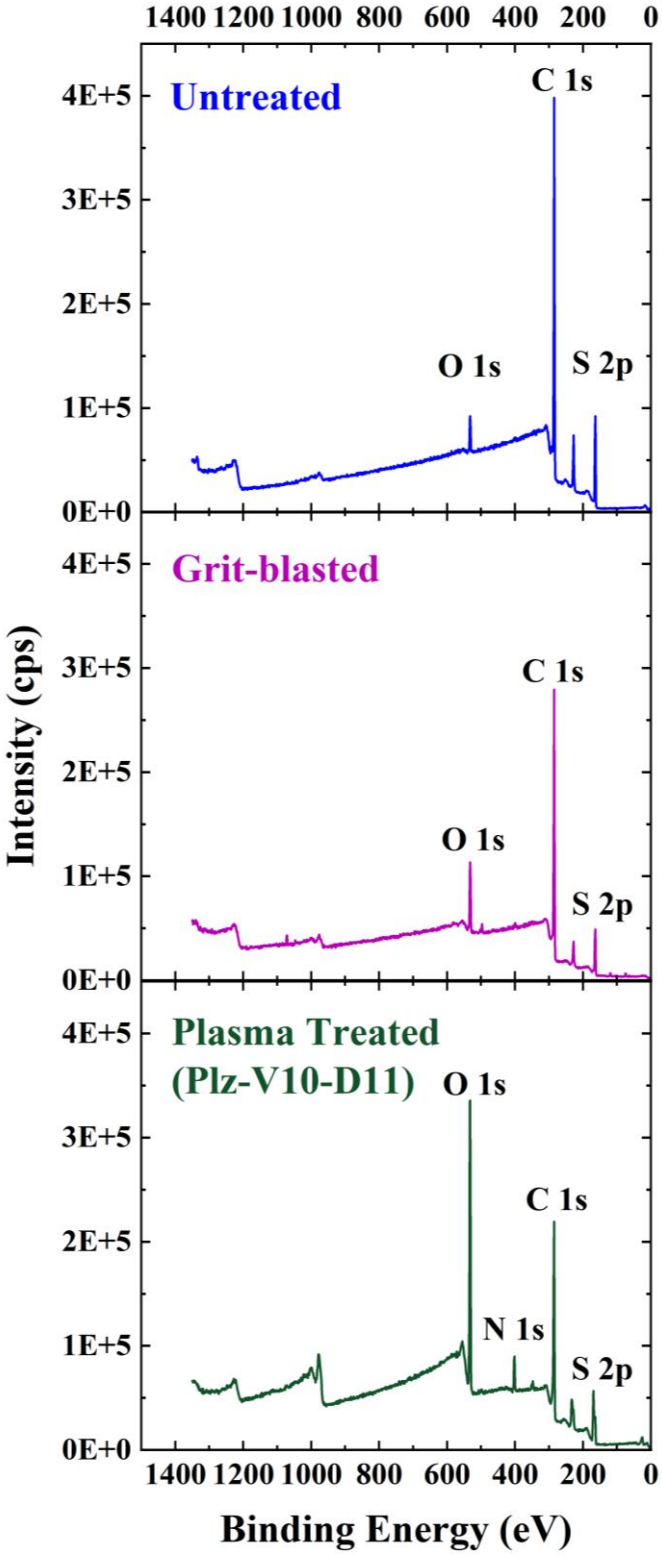

Figure 3.5 XPS spectra of the Untreated, Grit-blasted and one of the Plasma Treated (Plz-V10-D11) PPS/CF surfaces.

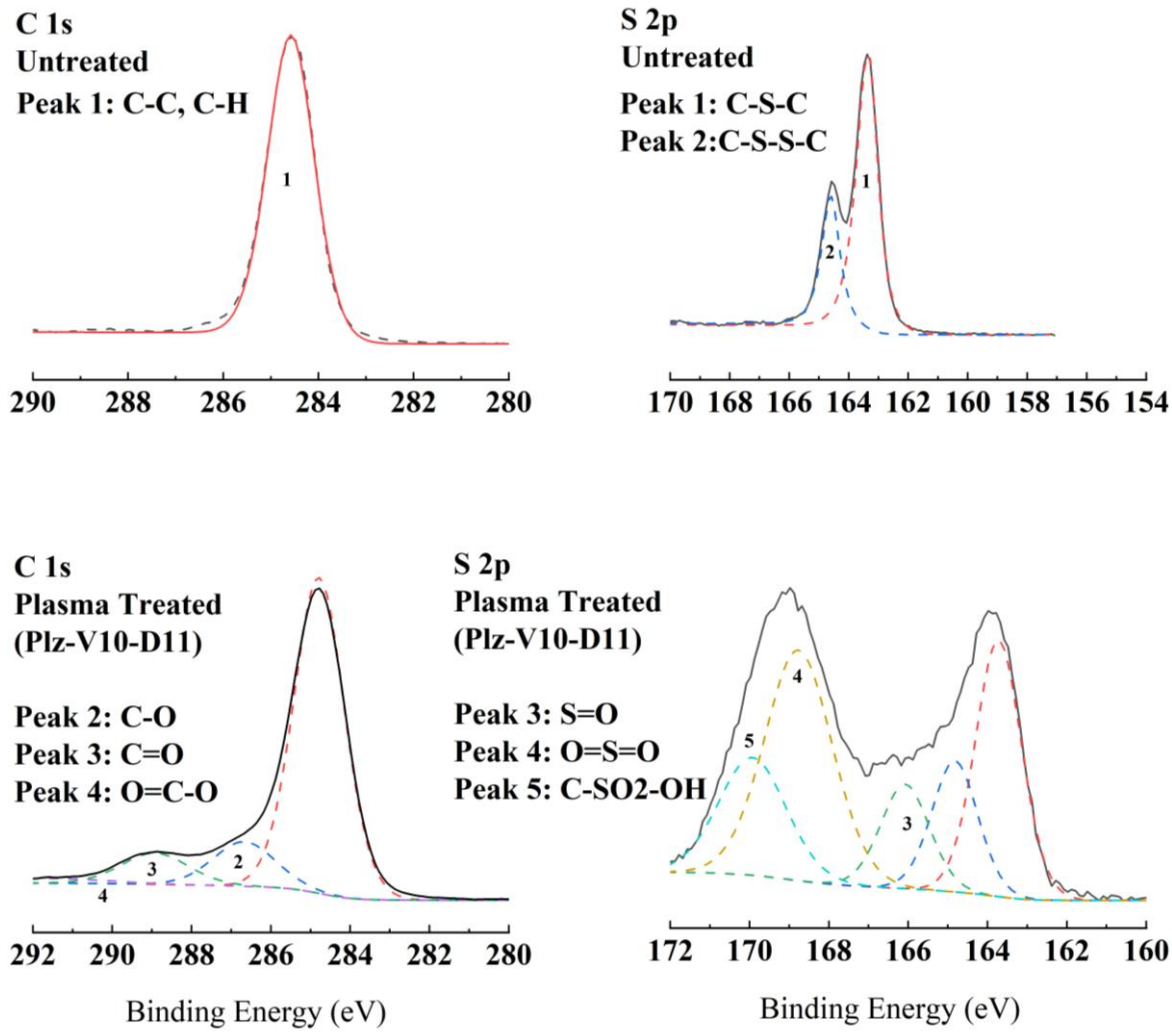

Figure 3.6 Deconvoluted forms of the C 1s and S 2p XPS spectra for the Untreated sample (above) and Plz-V10-D11 Plasma treated sample (below)

3.5 Structural Integrity and Matrix Crystallinity of PPS/CF Laminates Before and After Joining

In this study, as explained in Experimental Work section, there were two processing methods used; the first one was "Consolidation of Prepreg Layers" under Hot Press for the Production of PPS/CF Laminates, while the second one was "Autoclave Curing" of the Film Adhesive layer placed in between the two PPS/CF laminates for Joining. Alternatively, in this section, structures obtained after the first process could be named as "Before Joining", while the structures obtained after the second process as "After Joining". Thus, it was important to observe Structural Integrity and Matrix Crystallinity of PPS/CF laminate structures "Before" and "After" joining.

(i) *Ultrasonic Inspection*

In order to reveal whether there was formation of large scale voids or delamination between the layers, PPS/CF laminates both "before" and "after" joining, were inspected by an Automated Ultrasonic Through Transmission (AUTT) system. As illustrated in Figure 3.7, images obtained from this ultrasonic inspection system revealed that there was no significant damage in the PPS/CF laminate structures produced "before joining" and "after joining" of Untreated, Grit-blasted and Plasma treated surfaces. Dark regions seen at the edges of the images indicated that there was certain degree of defects formed at the edges of the laminates. However, this was not a problem, because edges of the laminates were all cut during specimen preparation for testing and analyses.

Thus, it could be stated that production of PPS/CF laminates and their Film Adhesive joining processes were both performed properly, without leading to large scale voids or delamination.

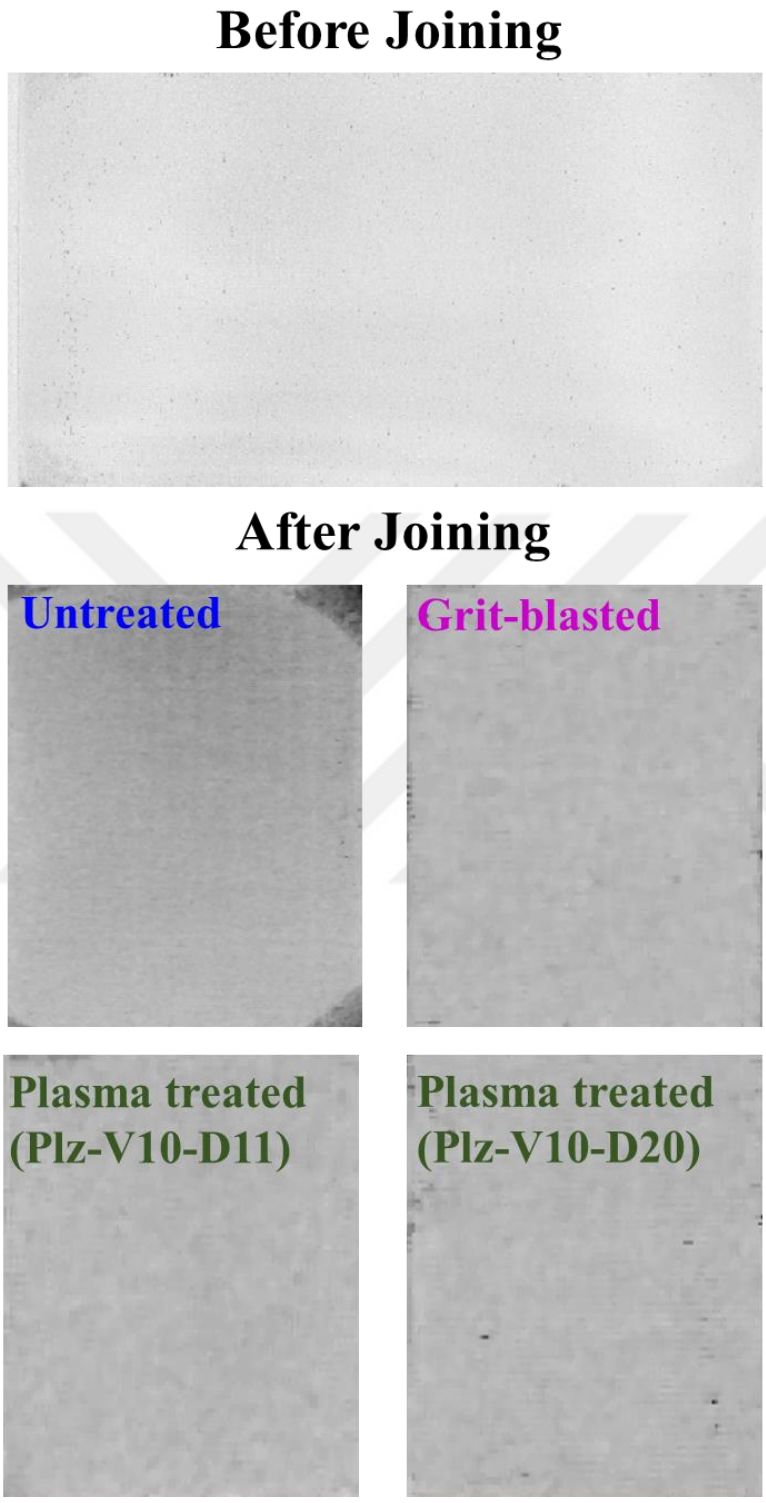

Figure 3.7 Examples of the Ultrasonic Inspection images of the PPS/CF laminates "before" joining, and "after" joining of Untreated, Grit-blasted and Plasma treated surfaces.

(ii) *DSC*

PPS matrix material of the composite laminates produced in this study was partially crystalline thermoplastic polymer having approximately 30% crystallinity. It is known that amount of crystallinity influences mechanical and thermal performance of thermoplastic polymers. Thus, in order to reveal whether there was significant decrease or not in the crystallinity degree of PPS matrix both "before" and "after" joining, DSC analyses were conducted for each case.

As shown in Figure 3.8, First Heating and Cooling thermograms of PPS/CF samples "before" and "after" joining indicated that values of temperatures for glass transition (T_g), crystallization (T_c) and melting (T_m) were around 88°C, 240°C and 285°C, respectively.

Moreover, during First Heating profile no cold crystallization enthalpy (ΔH_{cc}) was observed for each case, which would be interpreted that cooling rates used during these two processes (before and after joining) were sufficient for the crystallization of PPS macromolecular chains. Then, % crystallinity of PPS matrix for each case were determined by using the values of melting enthalpies (ΔH_m) only resulting in 28% for both "before" and "after" joining.

Thus, it could be pointed out that, heating and cooling parameters used during the production of PPS/CF laminates and their Film Adhesive joining processes have been both selected properly; leading to both 28% crystallinity, being very close to the expected crystallinity degree of around 30%.

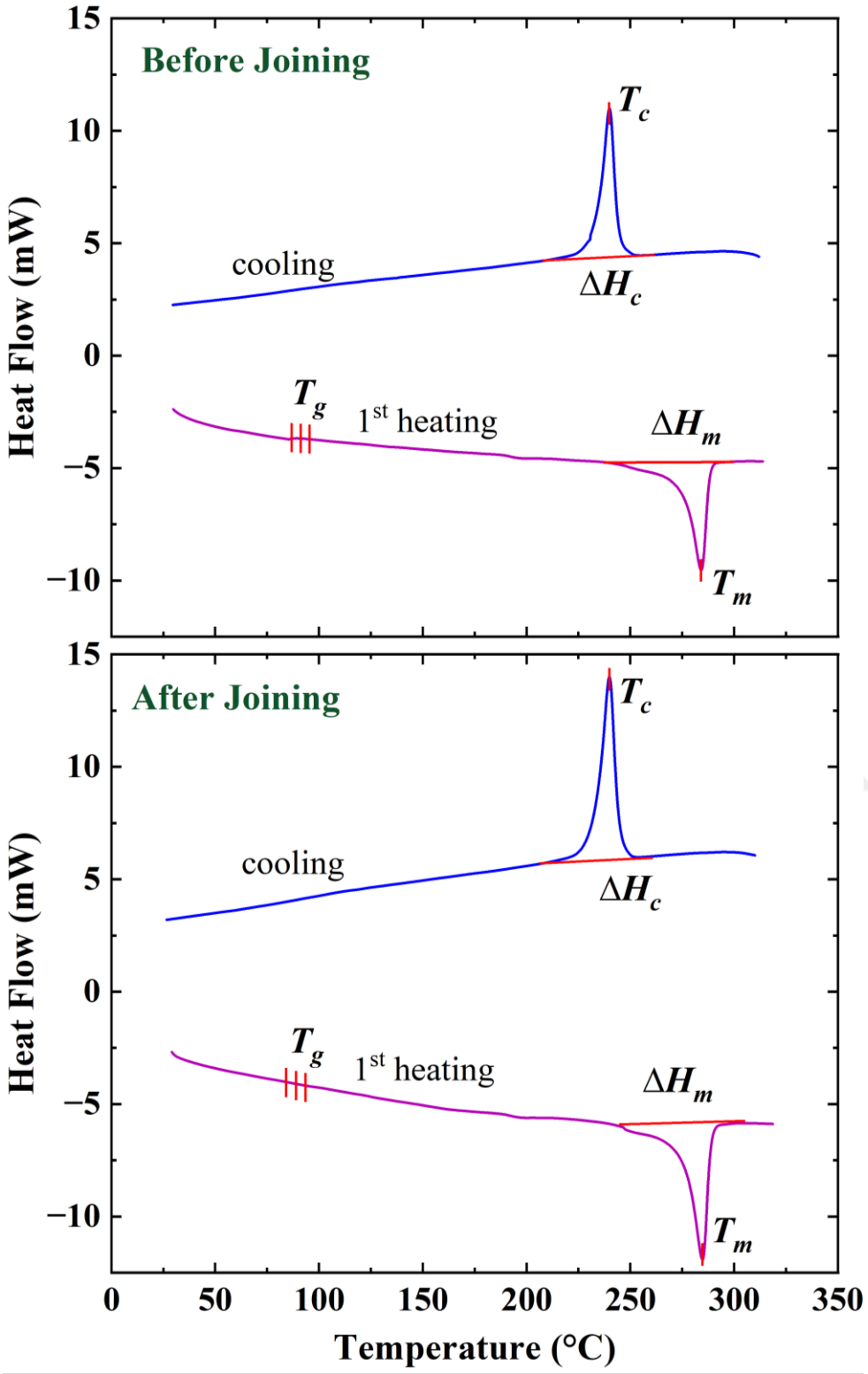

Figure 3.8 First Heating and Cooling DSC Thermograms of PPS/CF samples before and after Joining.

3.6 Effects of Plasma Treatment on the Interlaminar Shear Strength of Joined Specimens

It is known that [8, 54-56] one of the best testing method to determine Interlaminar Shear Strength and to observe Failure Modes of the Film Adhesive joined composite specimens is Single Lap Shear Strength (SLSS) tests. Thus, after obtaining Load-Displacement curves of all PPS/CF specimens "after" joining, their SLSS values were compared in Figure 3.9 and tabulated in Table 3.5. At the end, failure mode mechanisms of the specimens were also studied.

As shown in Figure 3.9, after Grit-blasting, it was observed that SLSS value of Untreated specimen increased from 6 MPa to 17 MPa, an increase of almost 3 times. That improvement was mainly due to the increased surface roughness leading to efficient mechanical interlocking mechanism at the interface. This is one of the reason why that conventional surface treatment is still used in the aircraft industry.

On the other hand, the improvement after plasma treatment was more significant. For instance for the Plz-V10-D11 specimen SLSS value increased up to 23 MPa, i.e. an increase of almost 4 times. Because, as discussed before, plasma treatment resulted in formation of oxidized functional groups on the surfaces of PPS/CF samples leading to efficient polar interactions and chemical bonding mechanisms at the interface.

Figure 3.9 also indicated that when Velocity and Distance parameters of plasma treatment were increased, due to the rather lower chemical interactions, SLSS values of the specimens decreased slightly. However, even the SLSS values of Plz-V10-D20 and Plz-V200-D11 specimens were still above the SLSS value of Grit-blasted specimen.

Depending on the joining quality of the Film Adhesive bonding, interlaminar failure might occur in certain modes. As schematically shown in Figure 3.10, three typical interlaminar "Failure Modes" could be observed: (i) Adhesive Failure, (ii) Cohesive Failure, and (iii) Mixed Failure.

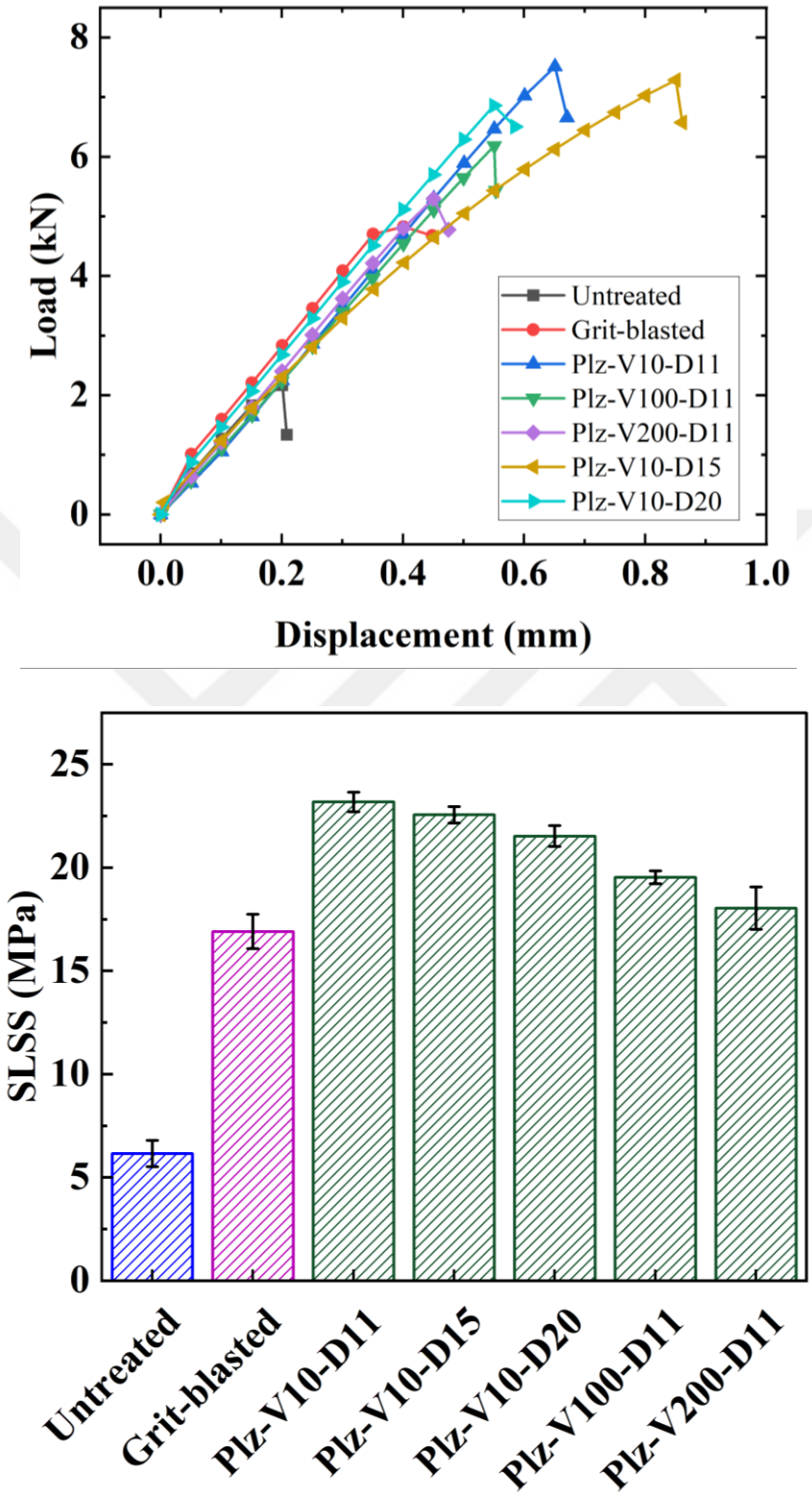

Figure 3.9 Load-Displacement curves and SLSS values of the Untreated, Grit-blasted and Plasma treated PPS/CF specimens after joining.

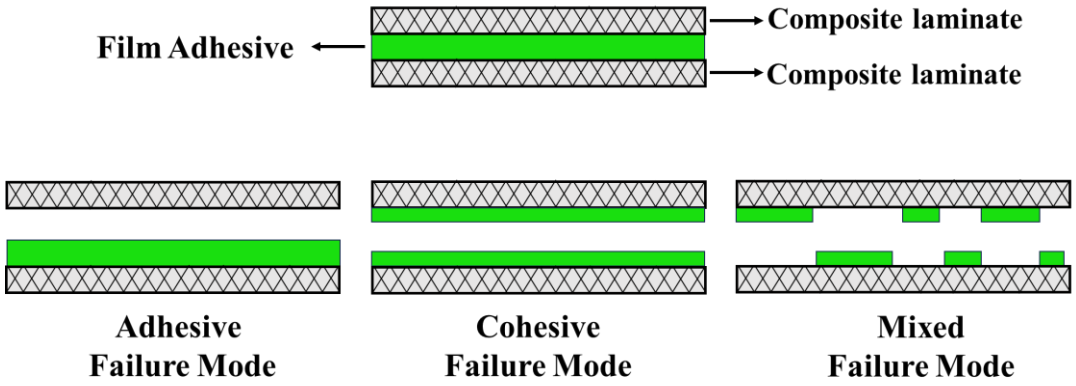

Figure 3.10 Schematics of Three Typical Interlaminar Failure Modes that could be observed in Film Adhesive Joining method.

"Adhesive Failure" is the interlaminar failure which takes place between the Composite Laminate and the Film Adhesive. In represents the lowest quality of the joining method, mainly due to the absence of any polar interactions or chemical bonding mechanisms at the interface. Thus, as shown in Figure 3.11, Adhesive Failure mode was observed for the Untreated PPS/CF specimens having the lowest SLSS value. It was clearly seen that green-colored Film Adhesive material remained on one side of the failure zone, the other side being free of Film Adhesive.

Contrarily, "Cohesive Failure" is the interlaminar failure which take place through the Film Adhesive material itself. It represents the highest quality of the joining method, mainly due to the significant degree of chemical bonding mechanism at the interface. Thus, as shown in Figure 3.11, Cohesive Failure mode was only observed in the Plasma treated PPS/CF specimens having the highest SLSS values. In this case, green-colored Film Adhesive material remained on both sides of the failure zone.

"Mixed Failure" could be designed as the mixture of Adhesive and Cohesive failure modes, i.e. the failure zone takes place partly Adhesive and partly Cohesive. It represents a moderate quality of the joining method, mainly due to mechanical interlocking mechanism and certain degree of polar interactions at the interface. As shown in Figure 3.11, this type of Mixed Failure mode was observed especially for

the Grit-blasted PPS/CF specimens having moderate level SLSS value. In this case, green-colored Film Adhesive material remained partly one side and partly on the other side of the failure zone.

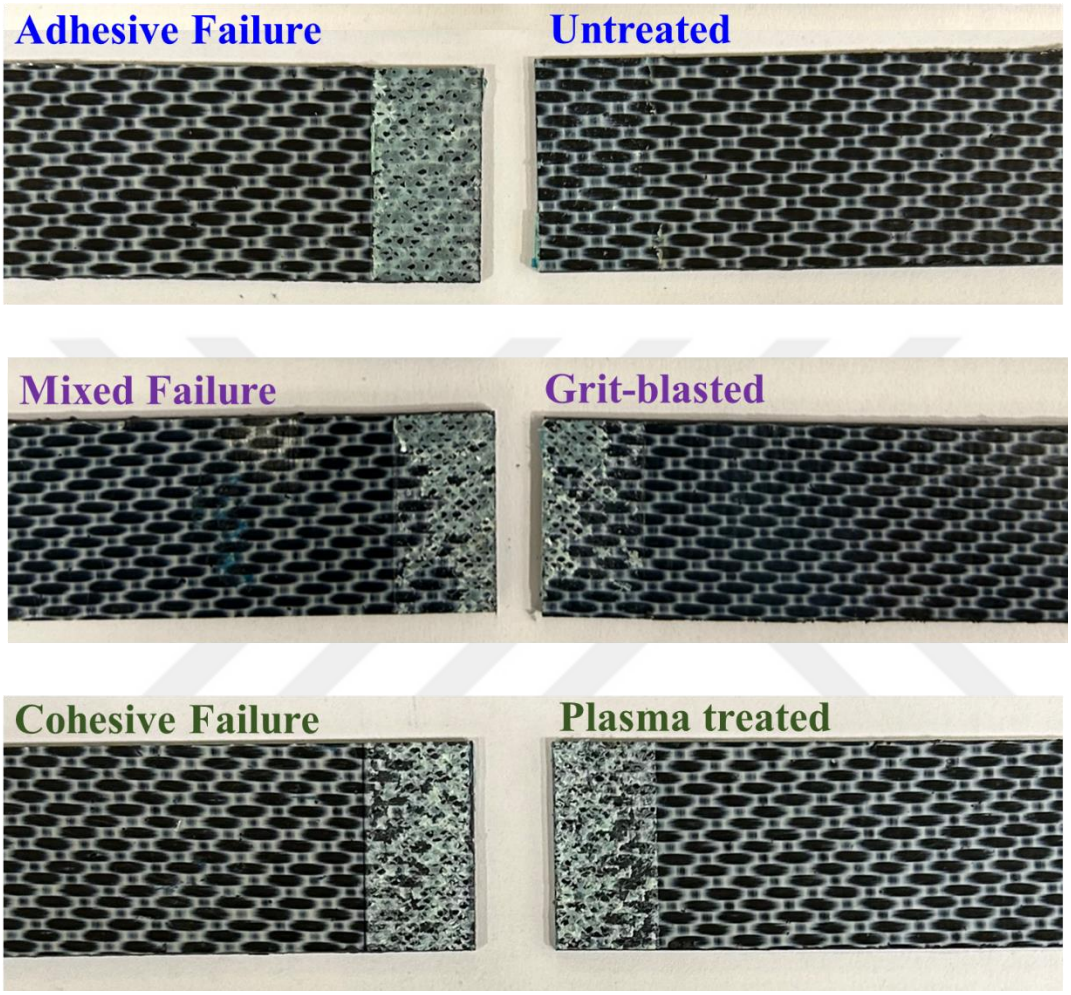

Figure 3.11 Examples of the three typical interlaminar failure modes observed during SLSS tests.

Table 3.5 Average values of the Interlaminar Shear Strength and Interlaminar Fracture Toughness Energy of the Specimens "after" joining.

	SLSS (MPa)	**G_{IC} (J/m^2)**
Untreated	6.16 ± 0.64	35.51 ± 4.07
Grit-blasted	16.91 ± 0.83	221.88 ± 5.01
Plz-V10-D11	23.18 ± 0.47	370.73 ± 9.91
Plz-V10-D15	22.56 ± 0.40	289.34 ± 10.1
Plz-V10-D20	21.53 ± 0.50	273.93 ± 7.95
Plz-V100-D11	19.53 ± 0.31	256.73 ± 12.5
Plz-V200-D11	18.04 ± 1.02	238.56 ± 8.12

3.7 Effects of Plasma Treatment on the Interlaminar Fracture Toughness of Joined Specimens

Another important mechanical test to determine especially resistance of the bonded interface against crack propagation or delamination is the Interlaminar Fracture Toughness Energy under Mode-I, i.e. G_{IC} test [16, 57, 58]. Thus, after obtaining Load-Displacement curves of all PPS/CF specimens "after" joining, their G_{IC} values were compared in Figure 3.12 and tabulated in Table 3.5.

As expected, it was observed that the trends in the results of G_{IC} tests were very similar to the trends in SLSS tests. Because, their bonding mechanisms discussed in the previous section were all the same. For example, after Grit-blasting G_{IC} value of Untreated specimen increased form 35 J/m^2 to 222 J/m^2, an increase of more than 6 times. The increase for the Plasma treated (Plz-V10-D11) specimen was up to 371 J/m^2, i.e. an increase of more than 10 times. Similarly, increasing the Velocity and Distance parameters of the Plasma treatment resulted in slight decreases in the values of G_{IC}, but still remaining above the G_{IC} value of Grit-blasted specimen.

Due to the same bonding mechanisms discussed before, it was revealed that three typical failure modes observed in SLSS tests were almost the same in G_{IC} tests. For

instance, Figure 3.13 indicated that “Adhesive Failure” occurred again in the Untreated specimen, “Cohesive Failure” occurred again in the Plasma treated specimens, while “Mixed Failure” occurred in the Grit-blasted specimen.

Therefore, it could be generally stated that due to the much higher interlaminar mechanical properties (both SLSS and G_{IC}) obtained in Plasma treated specimens, traditional Grit-blasting surface treatment could be replaced with Atmospheric Plasma surface treatment before Film Adhesive joining of PPS/CF composite parts in aircraft industry.

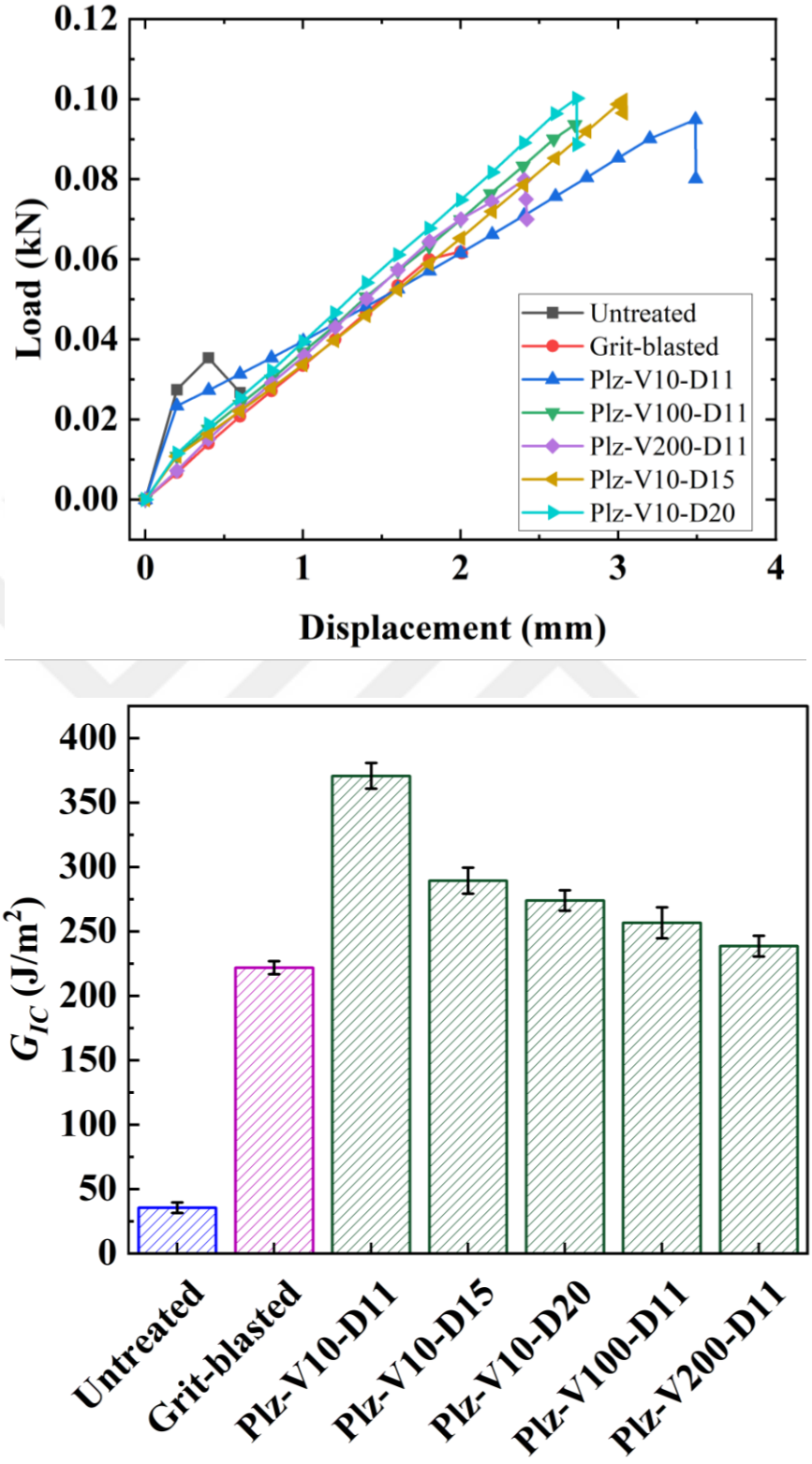

Figure 3.12 Load-Displacement curves and G_{IC} values of the Untreated, Grit-blasted and Plasma treated PPS/CF specimens after joining.



Figure 3.13 Examples of the three typical interlaminar failure modes observed during G_{IC} tests.

3.8 Effects of Plasma Treatment on the Drop-Weight Impact Toughness of Joined Specimens

For the composite laminate structures, Drop-Weight Impact test is a common method used to determine their Impact Toughness Energy absorbed and to observe dent and area of the damaged zone. On the other hand, there were very limited studies [59, 60] investigating the performance of composite parts joined by Adhesive Bonding methods; and none of them were for the PPS/CF laminates. Thus, as the first time in the literature, effects of surface treatments on the Film Adhesive joining performance of PPS/CF laminates were evaluated by also conducting Drop-Weight Impact test.

During the test, first "Contact Force versus Time" and "Absorbed Energy versus Time" curves were obtained. Examples of these curves were given in Figure 3.14. Then, maximum values of Contact Force (F_{max}) and Absorbed Energy (E_{max}) after all specimens were compared in Figure 3.15 and tabulated in Table 3.6.

It was seen that, just like SLSS and G_{IC} values discussed before, Grit-blasting increased F_{max} and E_{max} values of the Untreated specimen only slightly, whereas Plasma treatments resulted in significant increases being all more than 30%.

Then, Impact Toughness performance of all PPS/CF specimens were also evaluated by examining the damaged zone qualitatively and quantitatively. For this purpose, first of all top-view photographic images of all specimens were taken under visible light, then for more clear observation under UV light. Examples of these top-view images given in Figure 3.16 indicated that impact damage formed in the center of the specimens propagated in other directions mainly through matrix-rich regions.

For the quantitative damage analysis, "Dent Depth" i.e. penetration distance from the surface of the specimens were measured by using a digital dept indicator, and the results in mm were tabulated in Table 3.6.

After that, in order to measure "Damage Area" not only from the top-view images, but also through the thickness of the specimens; Automated Ultrasonic Through Transmission (AUTT) inspection technique was used. Examples of these through-

thickness ultrasonic images together with image analysis software views determining the Damage Area were given in Figure 3.17. Then, these Damage Area values in mm^2 were also tabulated in Table 3.6.

Table 3.6 revealed that both Dent Depth and Damage Area values of the Untreated specimens decreased only slightly after Grit-blasting. On the other hand, the decreases were more significant after all Plasma treatments.

Thus, it could be stated that replacement of Grit-blasting with Plasma surface treatment would be efficient also in terms of Impact Toughness performance of Film Adhesive joined PPS/CF structures.

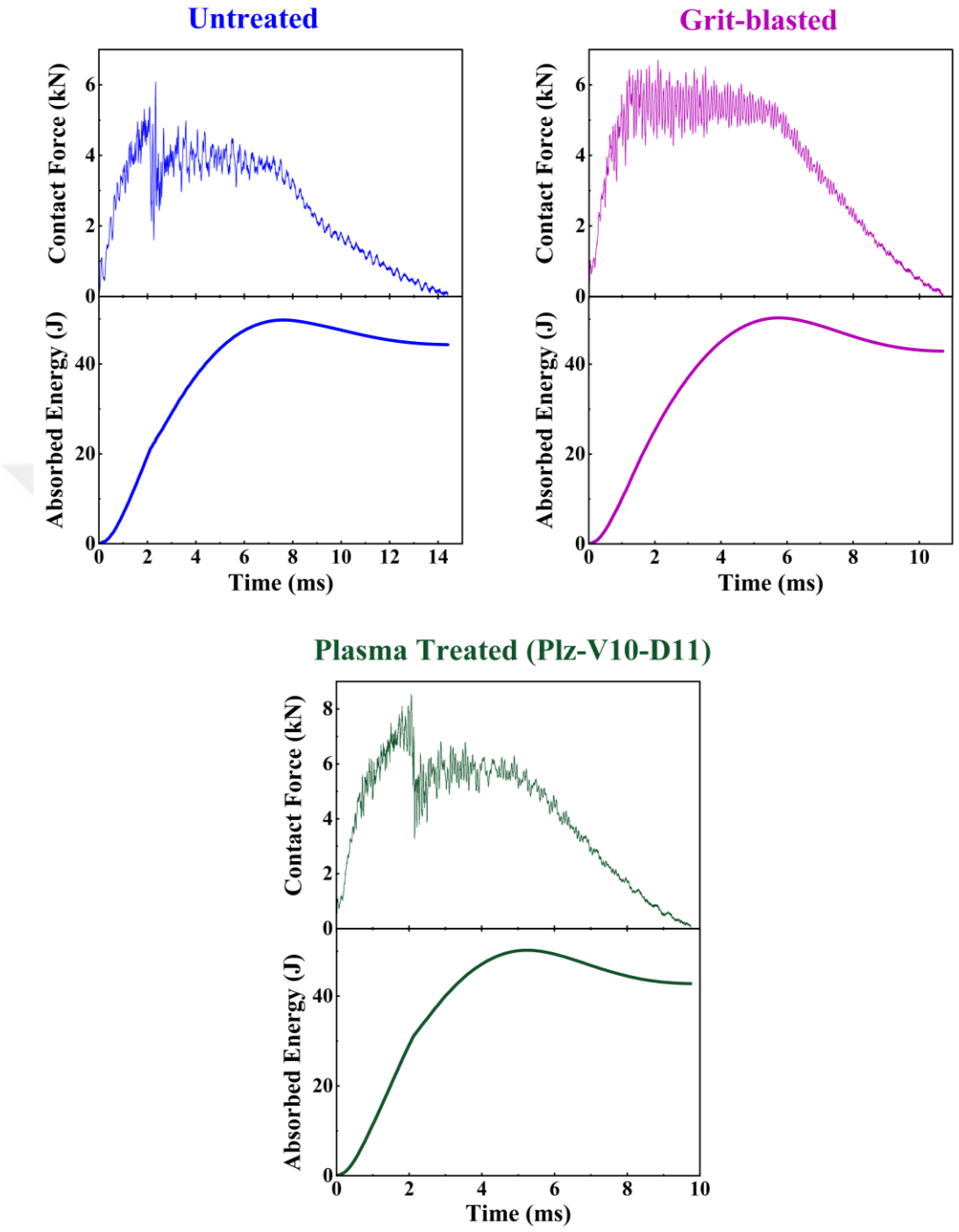

Figure 3.14 Examples of the "Contact Force versus Time" and "Absorbed Energy versus Time" curves obtained during Drop-Weight Impact tests of PPS/CF specimens after joining.

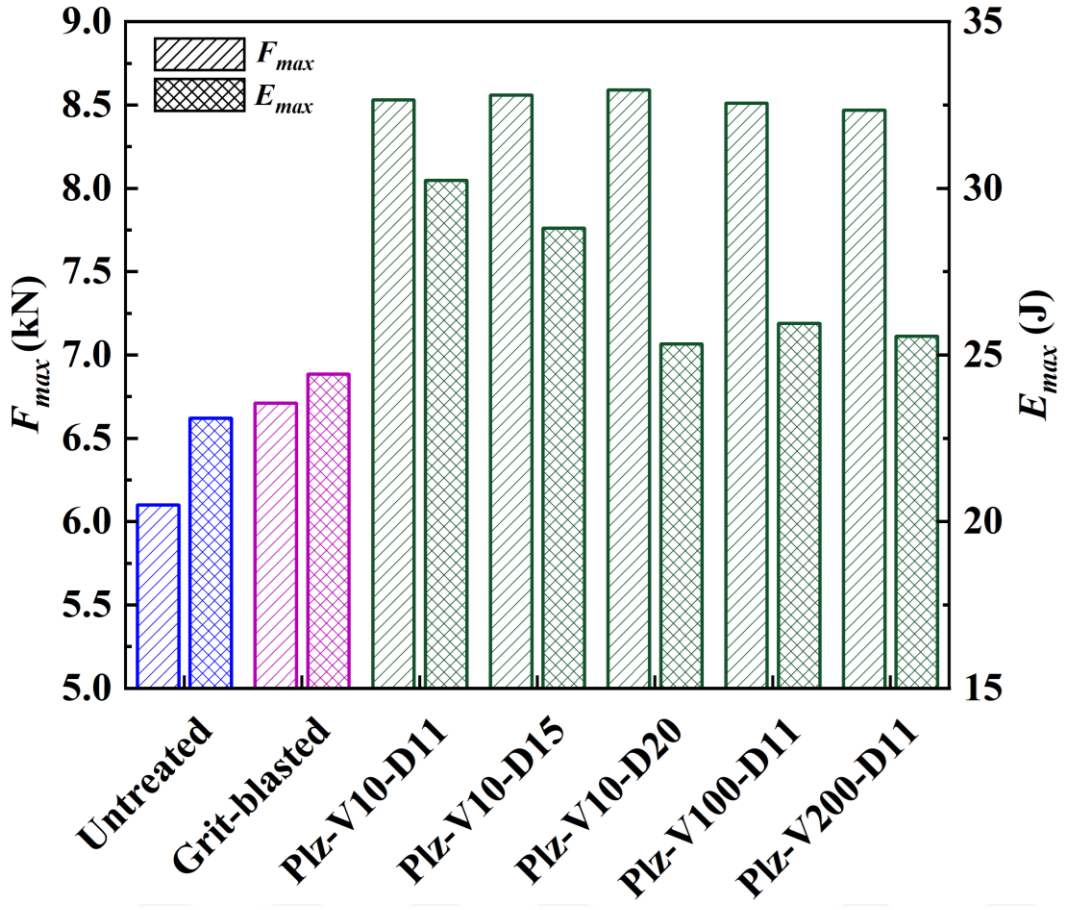

Figure 3.15 Maximum Contact Force (F_{max}) and Maximum Absorbed Energy (E_{max}) of the Untreated, Grit-blasted and Plasma treated PPS/CF specimens after Joining.

Table 3.6 Values of the Dent Depth, Damage Area, Maximum Contact Force (F_{max}) and Maximum Absorbed Energy (E_{max}) obtained from Drop-Weight Impact tests of Untreated, Grit-blasted and Plasma Treated PPS/CF specimens "after" joining.

	Dent Depth (mm)	**Damage Area (mm^2)**	**F_{max} (kN)**	**E_{max} (J)**
Untreated	1.92	3450	6.10	23.10
Grit Blasted	1.87	1443	6.71	24.43
Plz-V10-D11	1.44	1064	8.53	30.24
Plz-V10-D15	1.60	1109	8.56	28.80
Plz-V10-D20	1.74	1224	8.59	25.33
Plz-V100-D11	1.47	1324	8.51	25.95
Plz-V200-D11	1.48	1356	8.47	25.56

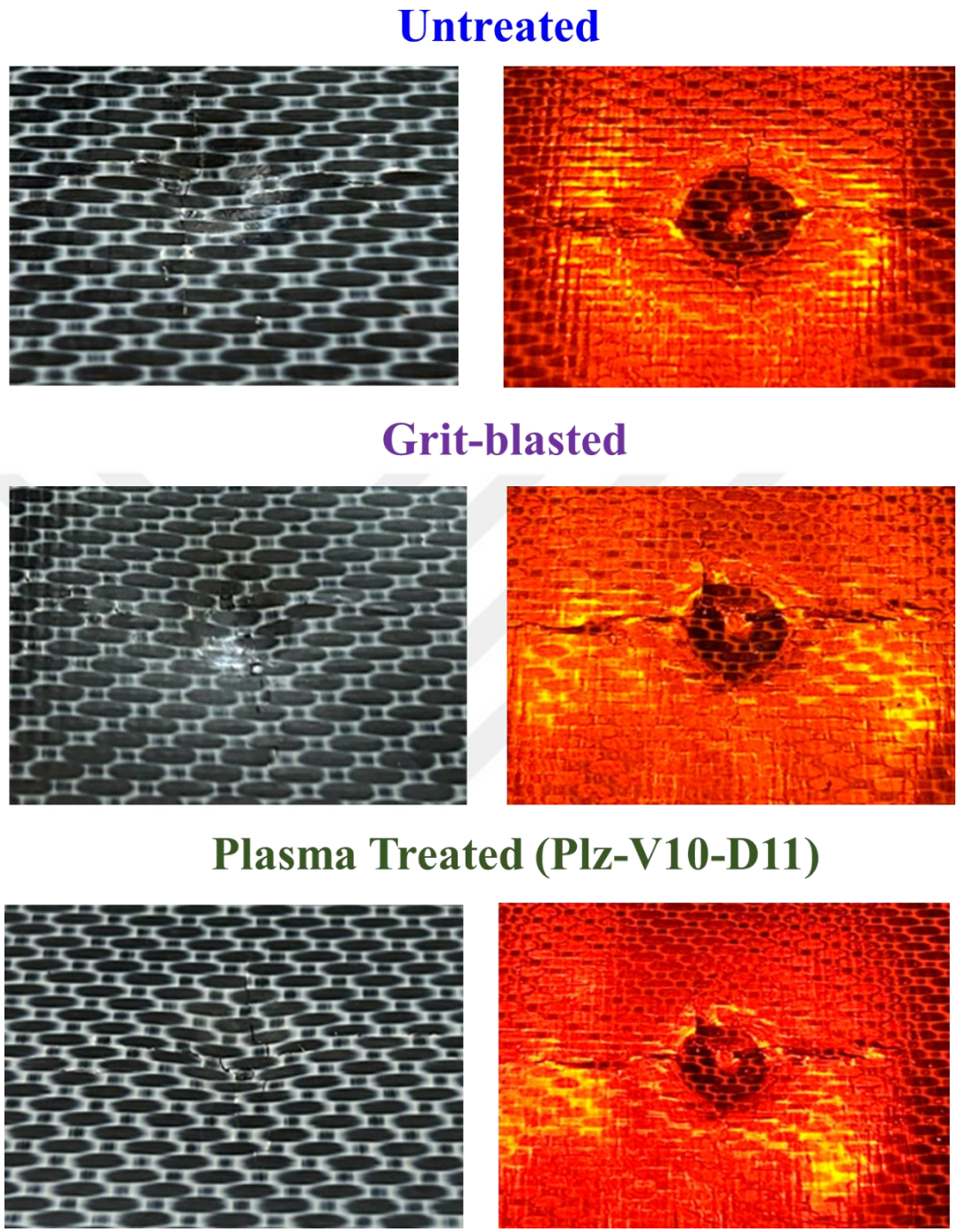

Figure 3.16 Examples of the Top-View Photographic Images taken under visible light (left) and UV light (right) of the Damage Zones occurred in the Drop-Weight Impact tests of PPS/CF specimens after joining.

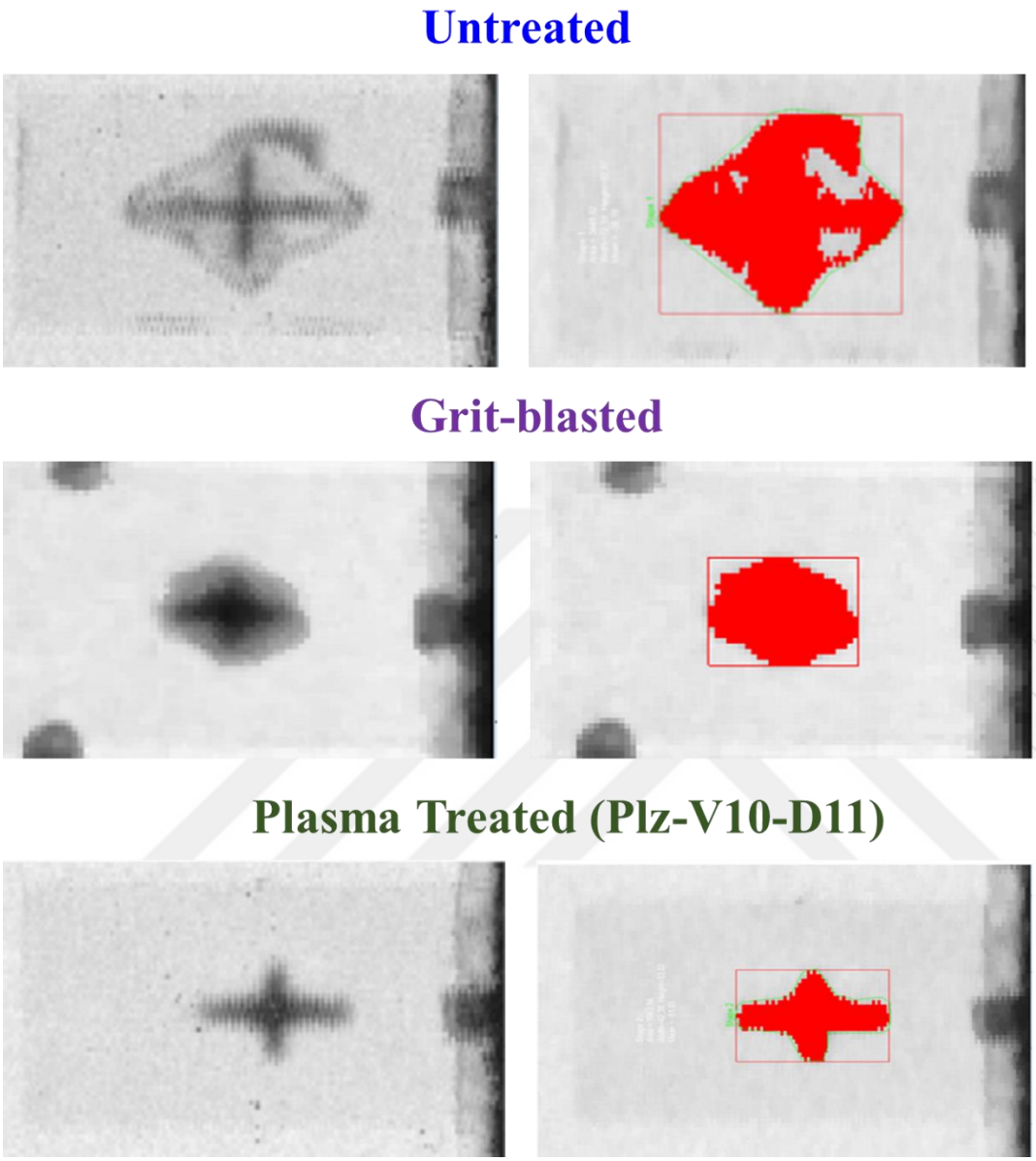

Figure 3.17 Examples of the through-thickness Ultrasonic Images together with Image Analyses Software area determination of the Damage Zones occurred in the Drop-Weight Impact tests of the PPS/CF specimens after joining.

CHAPTER 4

CONCLUSIONS

Main conclusions drawn from the Film Adhesive joining performance studies for PPS/CF thermoplastic composite laminates could be outlined as follows.

- Thermal camera analysis during plasma surface treatments revealed that selected plasma velocity and plasma distance parameters resulted in not more than 66°C surface temperature which was below the T_g of the PPS matrix; i.e., leading to no detrimental effects.

- Profilometer surface topography in terms of *Ra* and *Rz* indicated that traditional Grit-blasting surface treatment increased surface roughness of the specimens enormously, being more than 7 times; i.e., the dominant bonding mechanism in the Film Adhesive joining was mechanical interlocking.

- Wettability analysis in terms of Contact Angle and Surface Energy, chemical analysis in terms of FTIR and XPS all indicated that plasma surface treatment resulted in formation of chemically reactive sites, i.e., dominant bonding mechanisms in the Film Adhesive joining were certain polar interactions and chemical bonding.

- Before and after the joining process, Ultrasonic Inspection revealed that there was no formation of large-scale voids or delamination between the layers, while DSC analysis revealed that there was no change in the partial crystallinity amount of the thermoplastic matrix; i.e., it could be stated that production of PPS/CF laminates and their Film Adhesive joining processes were both performed properly.

- Mechanical tests in terms of SLSS, G_{IC} and Drop-Weight Impact all pointed out that compared to Grit-blasting, Plasma surface treatment resulted in considerably higher joint performance regarding Interlaminar Shear Strength, Interlaminar Fracture Toughness and Impact Toughness.

- It was also observed that Adhesive failure mode occurred in the Untreated specimen, Cohesive failure mode occurred in the Plasma treated specimens, while Mixed failure mode occurred in the Grit-blasted specimen.

Therefore, it could be generally concluded that due to the significant improvement in the joint performance obtained in Plasma treated specimens, traditional Grit-blasting surface treatment could be replaced with Atmospheric Plasma surface treatment before Film Adhesive joining of PPS/CF composite parts in aircraft industry.

REFERENCES

[1] M. G. Romano, M. Guida, F. Marulo, M. G. Auricchio, and S. Russo, "Characterization of adhesives bonding in aircraft structures," *Materials*, vol. 13, no. 21, pp. 1–13, Nov. 2020, doi: 10.3390/ma13214816.

[2] J. Zhang, M. de Souza, C. Creighton, and R. J. Varley, "New approaches to bonding thermoplastic and thermoset polymer composites," *Composites Part A: Applied Science and Manufacturing*, vol. 133, pp. 1–8, Jun. 2020, doi: 10.1016/j.compositesa.2020.105870.

[3] C. J. Li, X. T. Luo, S. W. Yao, G. R. Li, C. X. Li, and G. J. Yang, "The Bonding Formation during Thermal Spraying of Ceramic Coatings: A Review," *Journal of Thermal Spray Technology*, vol. 31, no. 4, pp. 780–817, Apr. 01, 2022. doi: 10.1007/s11666-022-01379-z.

[4] G. S. Chae, H. W. Park, J. H. Lee, and S. Shin, "Comparative study on the impact wedge-peel performance of epoxy-based structural adhesives modified with different toughening agents," *Polymers*, vol. 12, no. 7, pp. 1–15, Jul. 2020, doi: 10.3390/polym12071549.

[5] S. G. Prolongo, G. Del Rosario, and A. Ureña, "Comparative study on the adhesive properties of different epoxy resins," *International Journal of Adhesion and Adhesives*, vol. 26, no. 3, pp. 125–132, Jun. 2006, doi: 10.1016/j.ijadhadh.2005.02.004.

[6] G. Scarselli, C. Corcione, F. Nicassio, and A. Maffezzoli, "Adhesive joints with improved mechanical properties for aerospace applications," *International Journal of Adhesion and Adhesives*, vol. 75, pp. 174–180, Jun. 2017, doi: 10.1016/j.ijadhadh.2017.03.012.

[7] A. Higgins, “Adhesive bonding of aircraft structures,” *International Journal of Adhesion & Adhesives*, vol. 20, pp. 367–376, Jan. 2000, doi: 10.1016/S0143-7496(00)00006-3.

[8] S. Deng, L. Djukic, R. Paton, and L. Ye, “Thermoplastic-epoxy interactions and their potential applications in joining composite structures - A review,” *Composites Part A: Applied Science and Manufacturing*, vol. 68, pp. 121–132, Jan. 2015 doi: 10.1016/j.compositesa.2014.09.027.

[9] F. J. Boerio, B. Roby, R. G. Dillingham, R. H. Bossi, and R. L. Crane, “Effect of grit-blasting on the surface energy of graphite/epoxy composites,” *Journal of Adhesion*, vol. 82, no. 1, pp. 19–37, Jan. 2006, doi: 10.1080/00218460500418516.

[10] R. J. Zaldivar, G. L. Steckel, B. A. Morgan, J. P. Nokes, and H. I. Kim, “Bonding optimization on composite surfaces using atmospheric plasma treatment,” *Journal of Adhesion Science and Technology*, vol. 26, no. 1–3, pp. 381–401, Jan. 2012, doi: 10.1163/016942411X576554.

[11] M. Noeske, J. Degenhardt, S. Strudthoff, and U. Lommatzsch, “Plasma jet treatment of five polymers at atmospheric pressure: Surface modifications and the relevance for adhesion,” *International Journal of Adhesion and Adhesives*, vol. 24, no. 2, pp. 171–177, Apr. 2004, doi: 10.1016/j.ijadhadh.2003.09.006.

[12] K. Sudheendra, J. Vinodhini, M. Govindaraju, and S. Bhowmik, “Comparative studies of nitrogen plasma and argon plasma treatment on the strength of PBO fibre reinforced high-temperature resistant thermoplastic composite,” *High Performance Polymers*, vol. 33, no. 7, pp. 729–740, Sep. 2021, doi: 10.1177/0954008320987296.

[13] C. Sun, J. Min, J. Lin, and H. Wan, “Effect of atmospheric pressure plasma treatment on adhesive bonding of carbon fiber reinforced polymer,” *Polymers*, vol. 11, no. 1, Jan. 2019, pp. 139 doi: 10.3390/polym11010139.

[14] R. Chamochin, M. C. De Santayana, J. Abenojar, M. Pantoja, Y. Ballesteros, and J. C. Del Real, “The effect of surface treatment on the behavior of toughened

acrylic adhesive/GRP (epoxy) composite joints," *Journal of Adhesion Science and Technology*, vol. 24, no. 11-12, Aug. 2010, pp. 1903–1916. doi: 10.1163/016942410X507641.

[15] J. W. Chin and J. P. Wightman, "Surface characterization and adhesive bonding of toughened bismaleimide composites," *Composites Part A: Applied Science and Manufacturing*, vol.27, no. 6, 1996, pp. 419–428, doi: 10.1016/1359-835X(95)00064-9.

[16] J. C. Del Real, Y. Ballesteros, R. Chamochin, J. Abenojar, and L. Molisani, "Influence of surface preparation on the fracture behavior of acrylic adhesive/CFRP composite joints," *Journal of Adhesion*, vol. 87, no. 4, pp. 366–381, Apr. 2011, doi: 10.1080/00218464.2011.562114.

[17] C. Dighton, A. Rezai, S. L. Ogin, and J. F. Watts, "Atmospheric plasma treatment of CFRP composites to enhance structural bonding investigated using surface analytical techniques," *International Journal of Adhesion and Adhesives*, vol. 91, pp. 142–149, Jun. 2019, doi: 10.1016/j.ijadhadh.2019.03.010.

[18] J. Lin, C. Sun, J. Min, H. Wan, and S. Wang, "Effect of atmospheric pressure plasma treatment on surface physicochemical properties of carbon fiber reinforced polymer and its interfacial bonding strength with adhesive," *Composites Part B: Engineering*, vol. 199, pp. 1–12, Oct. 2020, doi: 10.1016/j.compositesb.2020.108237.

[19] J. Mohan, A. Ramamoorthy, A. I. Ivankovic, D. Dowling, and N. Murphy, "Effect of an atmospheric pressure plasma treatment on the mode I fracture toughness of a co-cured composite joint," *The Journal of Adhesion*, vol. 90, no. 9, pp. 733–754, Apr. 2014, doi: 10.1080/00218464.2013.772053

[20] J. Li, Y. Yan, T. Zhang, and Z. Liang, "Experimental study of adhesively bonded CFRP joints subjected to tensile loads," *International Journal of Adhesion and Adhesives*, vol. 57, pp. 95–104, Mar. 2015, doi: 10.1016/j.ijadhadh.2014.11.001.

[21] K. Ma, P. Chen, B. Wang, G. Cui, and X. Xu, "A study of the effect of oxygen plasma treatment on the interfacial properties of carbon fiber/epoxy composites," *Journal of Applied Polymer Science*, vol. 118, no. 3, pp. 1606–1614, Nov. 2010, doi: 10.1002/app.32549.

[22] S. G. Prolongo, M. R. Gude, G. Del Rosario, and A. Ureña, "Surface pretreatments for composite joints: Study of surface profile by SEM image analysis," *Journal of Adhesion Science and Technology*, vol. 24, Aug. 2010, pp. 1855–1867. doi: 10.1163/016942410X507623.

[23] M. Pizzorni, E. Lertora, C. Gambaro, C. Mandolfino, M. Salerno, and M. Prato, "Low-pressure plasma treatment of CFRP substrates for epoxy-adhesive bonding: an investigation of the effect of various process gases," *International Journal of Advanced Manufacturing Technology*, vol. 102, no. 9–12, pp. 3021–3035, Jun. 2019, doi: 10.1007/s00170-019-03350-9.

[24] T. S. Williams, H. Yu, P. C. Yeh, J. M. Yang, and R. F. Hicks, "Atmospheric pressure plasma effects on the adhesive bonding properties of stainless steel and epoxy composites," *Journal of Composite Materials*, vol. 48, no. 2, pp. 219–233, Jan. 2014, doi: 10.1177/0021998312470150.

[25] R. J. Zaldivar, H. I. Kim, G. L. Steckel, J. P. Nokes, and B. A. Morgan, "Effect of processing parameter changes on the adhesion of plasma-treated carbon fiber reinforced epoxy composites," *Journal of Composite Materials*, vol. 44, no. 12, pp. 1435–1453, Jun. 2010, doi: 10.1177/0021998309355846.

[26] L. Wen, X. Xu, and L. Qin, "Effect of Low-Temperature Plasma Surface Treatment on Bonding Properties of Single-Lap Joint of Thermosetting Composites," *Polymers*, vol. 15, no. 7, pp. 1–24, Apr. 2023, doi: 10.3390/polym15071631.

[27] C. Palleiro, E. Rodríguez-Senín, R. Losada, and R. De La Mano, "*Study of the adhesive bonding of a thermoplastic composite material based on polypropylene*

and glass fiber," Proceedings of the 16th European Conference on Composite Materials–ECCM 16, Seville, Spain, 8 pages, (22-26 June 2014).

[28] E. Occhiello, G. Guerrini, and F. Garbassi, "Adhesion properties of plasma-treated carbon/PEEK composites," *Composites*, vol. 23, no. 3, pp. 193–200, May. 1992, doi: 10.1016/0010-4361(92)90440-6.

[29] R. Hicks, S. Babayan, J. Penelon, Q. Truong, D. Cheng, V. Le, J. Ghilarducci, A. Hsieh, J. Deitzel and J. Gillespie, "*Atmospheric Plasma Treatment of Polyetheretherketone Composites for Improved Adhesion*," Proceedings of the SAMPE Fall Technical Conference, Global Advances in Materials and Process Engineering, Dallas, Texas, USA, 9 pages on CD-ROM, (6-9 November 2006).

[30] N. Anagreh, L. Dorn, and C. Bilke-Krause, "Low-pressure plasma pretreatment of polyphenylene sulfide (PPS) surfaces for adhesive bonding," *International Journal of Adhesion and Adhesives*, vol. 28, no. 1–2, pp. 16–22, Jan. 2008, doi: 10.1016/j.ijadhadh.2007.03.003.

[31] W. Leahy, V. Barron, M. Buggy, T. Young, A. Mas, F. Schue, T. McCabe, and M. Bridge, "Plasma surface treatment of aerospace materials for enhanced adhesive bonding," *Journal of Adhesion*, vol. 77, no. 3, pp. 215–249, Aug. 2001, doi: 10.1080/00218460108030739.

[32] B. R. K. Blackman, A. J. Kinloch, and F. Watts, "The plasma treatment of thermoplastic fibre composites for adhesive bonding," *Composites*, vol. 25, no. 5, pp. 332–341, May. 1994, doi: 10.1016/S0010-4361(94)80003-0

[33] H. M. S. Iqbal, S. Bhowmik, and R. Benedictus, "Surface modification of high performance polymers by atmospheric pressure plasma and failure mechanism of adhesive bonded joints," *International Journal of Adhesion and Adhesives*, vol. 30, no. 6, pp. 418–424, Apr. 2010, doi: 10.1016/j.ijadhadh.2010.02.007.

[34] G. Scarselli, D. Quan, N. Murphy, B. Deegan, D. Dowling, and A. Ivankovic, "Adhesion Improvement of Thermoplastics-Based Composites by Atmospheric

Plasma and UV Treatments," *Applied Composite Materials*, vol. 28, no. 1, pp. 71–89, Feb. 2021, doi: 10.1007/s10443-020-09854-y.

[35] A. R. Chadwick, K. Kotzur, and S. Nowotny, "Moderation of thermoplastic composite crystallinity and mechanical properties through in situ manufacturing and post-manufacturing tempering: Part 1 – Mechanical characterisation," *Composites Part A: Applied Science and Manufacturing*, vol. 143, pp. 1–9, Apr. 2021, doi: 10.1016/j.compositesa.2021.106286.

[36] P. Berlin, O. Dickman and F. Larsson, "Effects of heat radiation on carbon/PEEK, carbon/epoxy and glass/epoxy composites," *Composites*, vol. 23, no. 4, pp. 235–243, Jul. 1992, doi: 10.1016/0010-4361(92)90183-U.

[37] M. Berczeli and Z. Weltsch, "Enhanced Wetting and Adhesive Properties by Atmospheric Pressure Plasma Surface Treatment Methods and Investigation Processes on the Influencing Parameters on HIPS Polymer," *Polymers*, vol. 13, no. 6, pp. 1–13, Feb. 2021, doi: 10.3390/polym13060901.

[38] B. G. Cho, S. H. Hwang, M. Park, J. K. Park, Y. Bin Park, and H. G. Chae, "The effects of plasma surface treatment on the mechanical properties of polycarbonate/carbon nanotube/carbon fiber composites," *Composites Part B: Engineering*, vol. 160, pp. 436–445, Mar. 2019, doi: 10.1016/j.compositesb.2018.12.062.

[39] F. Fanelli and F. Fracassi, "Atmospheric pressure non-equilibrium plasma jet technology: general features, specificities and applications in surface processing of materials," *Surface and Coatings Technology*, vol. 322, pp. 174–201, Aug. 2017, doi: 10.1016/j.surfcoat.2017.05.027.

[40] C. Ma, L. Wang, A. Nikiforov, Y. Onyshchenko, P. Cools, K. Ostrikov, N. De. Geyter and R. Morent, "Atmospheric-pressure plasma assisted engineering of polymer surfaces: From high hydrophobicity to superhydrophilicity," *Applied Surface Science*, vol. 535, pp. 1–12, Jan. 2021, doi: 10.1016/j.apsusc.2020.147032.

[41] G. Poletti, F. Orsini, A. Raffaele-Addamo, C. Riccardi, and E. Selli, “Cold plasma treatment of PET fabrics: AFM surface morphology characterisation,” *Applied Surface Science*, vol. 219, no. 3–4, pp. 311–316, Dec. 2003, doi: 10.1016/S0169-4332(03)00703-7.

[42] K. J. Kubiak, M. C. T. Wilson, T. G. Mathia, and P. Carval, “Wettability versus roughness of engineering surfaces,” *Wear*, vol. 271, no. 3–4, pp. 523–528, Jun. 2011, doi: 10.1016/j.wear.2010.03.029.

[43] R. Ourahmoune, M. Salvia, T. G. Mathia, and N. Mesrati, “Surface morphology and wettability of sandblasted PEEK and its composites,” *Scanning*, vol. 36, no. 1, pp. 64–75, Jan. 2014, doi: 10.1002/sca.21089.

[44] N. Manente André, S. M. Goushegir, N. Scharnagl, J. F. dos Santos, L. B. Canto, and S. T. Amancio-Filho, “Composite surface pre-treatments: Improvement on adhesion mechanisms and mechanical performance of metal–composite friction spot joints with additional film interlayer,” *Journal of Adhesion*, vol. 94, no. 9, pp. 723–742, Jul. 2018. doi: 10.1080/00218464.2017.1378101.

[45] H. Al-Maliki, L. Zsidai, P. Samyn, Z. Szakál, R. Keresztes, and G. Kalácska, “Effects of atmospheric plasma treatment on adhesion and tribology of aromatic thermoplastic polymers,” *Polymer Engineering and Science*, vol. 58, pp. 93–103, May. 2018, doi: 10.1002/pen.24689.

[46] H. Al-Maliki, L. Zsidai, P. Samyn, Z. Szakál, R. Keresztes, and G. Kalácska, “Effects of atmospheric plasma treatment on adhesion and tribology of aromatic thermoplastic polymers,” *Polymer Engineering and Science*, vol. 58, pp. 93–103, May 2018, doi: 10.1002/pen.24689.

[47] Z. Peiyuan, A. Tcharkhtchi, M. Shirinbayan, J. Fitoussi, F. Bakir, and F. B. Multiscale, “Multiscale physicochemical characterization of a short glass fiber-reinforced polyphenylene sulfide composite under aging and its thermo-oxidative mechanism,” *Polymers for Advanced Technologies*, vol. 30, pp. 1–11, Nov. 2018, doi: 10.1002/pat.4495.

[48] N. Kumar, S. K. Shukla, P. Tandon, and V. D. Gupta, “Vibrational spectroscopic investigation of Poly(p-phenylene sulfide),” *Journal of Polymer Science, Part B: Polymer Physics*, vol. 47, no. 23, pp. 2353–2367, Dec. 2009, doi: 10.1002/polb.21833.

[49] N. L. Batista, M. C. M. De Faria, K. Iha, P. C. De Oliveira, and E. C. Botelho, “Influence of water immersion and ultraviolet weathering on mechanical and viscoelastic properties of polyphenylene sulfide-carbon fiber composites,” *Journal of Thermoplastic Composite Materials*, vol. 28, no. 3, pp. 340–356, Mar. 2015, doi: 10.1177/0892705713484747.

[50] Z. Sun, L. Sun, C. Zhu, W. Tian, L. Shao, X. Feng and K. Huang, “Effect of Polyphenylene Sulphide Particles and Films on the Properties of Polyphenylene Sulphide Composites,” *Materials*, vol. 15, no. 21, pp. 1–13, Nov. 2022, doi: 10.3390/ma15217616.

[51] A. E. Abusrafa, S. Habib, I. Krupa, M. Ouederni, and A. Popelka, “Modification of polyethylene by RF plasma in different/mixture gases,” *Coatings*, vol. 9, no. 2, pp. 1–24, Jan. 2019, doi: 10.3390/COATINGS9020145.

[52] D. Xu, B. Liu, G. Zhang, S. Long, X. Wang, and J. Yang, “Effect of air plasma treatment on interfacial shear strength of carbon fiber-reinforced polyphenylene sulfide,” *High Performance Polymers*, vol. 28, no. 4, pp. 411–424, May. 2016, doi: 10.1177/0954008315585012.

[53] C. Lu, S. Qui, X. Lu, J. Wang, L. Xiao, T. Zheng, X. Wang, and D. Zhang, “Enhancing the interfacial strength of carbon fiber/poly(ether ether ketone) hybrid composites by plasma treatments,” *Polymers*, vol. 11, no. 5, pp. 1–15, May 2019, doi: 10.3390/polym11050753.

[54] A. Redmann, V. Damodaran, F. Tischer, P. Prabhakar, and T. A. Osswald, “Evaluation of single-lap and block shear test methods in adhesively bonded composite joints,” *Journal of Composites Science*, vol. 5, no. 1, pp. 1–13, Jan. 2021, doi: 10.3390/jcs5010027.

[55] J. Y. Cognard, R. Créachcadec, and J. Maurice, “Numerical analysis of the stress distribution in single-lap shear tests under elastic assumption - Application to the optimisation of the mechanical behaviour,” *International Journal of Adhesion and Adhesives*, vol. 31, no. 7, pp. 715–724, Oct. 2011, doi: 10.1016/j.ijadhadh.2011.07.001.

[56] M. D. Banea and L. F. M. Da Silva, “Adhesively bonded joints in composite materials: An overview,” *Proceedings of the Institution of Mechanical Engineers, Part L: Journal of Materials: Design and Applications*, vol. 223, no. 1. pp. 1–18, Jan. 01, 2009. doi: 10.1243/14644207JMDA219.

[57] H. B. Kim, K. Naito, and H. Oguma, “Fracture toughness of adherends bonded with two-part acrylic-based adhesive: Double cantilever beam tests under static loading,” *Applied Adhesion Science*, vol. 4, no. 1, pp. 1–11, Jun. 2016, doi: 10.1186/s40563-016-0067-3.

[58] D. Quan, R. Alderliesten, C. Dransfeld, I. Tsakoniatis, S. F. Teixeira, G. Scarselli, N. Murphy, A. Ivanković and R. Benedictus, “Significantly enhanced structural integrity of adhesively bonded PPS and PEEK composite joints by rapidly UV-irradiating the substrates,” *Composites Science and Technology*, vol. 199, pp. 1–11, Oct. 2020, doi: 10.1016/j.compscitech.2020.108358.

[59] Ramakrishna Pillai, G. (2006). *Response of adhesively bonded composite joints to low velocity impact*, (Doctoral dissertation, Wichita State University).

[60] Z. A. Aga and E. Woldesenbet, “Surface preparation effect on performance of adhesively-bonded graphite/epoxy composites subjected to impact,” Journal of Adhesion Science and Technology, vol. 21, no. 1, pp. 51–65, 2007, doi: 10.1163/15685610777997613.